

Three-Field String Inflation with Perturbative Corrections: Dynamics and Implications

Vasileios Basiouris^{◇ 1}, Dibya Chakraborty^{★ 2}

◇ *Physics Department, University of Ioannina
45110, Ioannina, Greece*

★ *Centre for Strings, Gravitation and Cosmology
Department of Physics, Indian Institute of Technology Madras,
Chennai 600036, India*

In this work, we construct an explicit string motivated example of three-field inflation in a related, yet distinct from, the recently discovered perturbative large volume scenario (pLVS). Contrary to the usual constructions, in this set up, large volume is ensured by the interplay between the effects of α^3 , logarithmic loop and higher derivative F^4 corrections. After addressing a full moduli stabilization scenario, we move on to a detailed analysis of three-field model of inflation after choosing a suitable canonical basis for the fields. We conduct multiple consistency checks to establish a solid foundation for our model within the framework of the underlying 4D effective field theory (EFT). Our model differs from previous setups in three key aspects: first, the interaction between subleading corrections that drive full moduli stabilization follows a different pattern, second, the volume form of the underlying Calabi-Yau is different, and third, in our three-field inflation scenario, the second slow-roll parameter consistently dominates over the first by several orders of magnitude. The latter signals the possible presence of primordial features which can be verified by forthcoming ground and space based experiments. We can roughly distinguish two stages of inflation: the first stage mostly occurs in the steepest direction during horizon crossing giving us almost 55 efolds of inflation—once one of the inflatons falls off the ridge and then to its true minimum, the other two fields become active, giving us a truly multi-field behavior in the second stage – adding few more efolds of inflation. We also confirm our claim by introducing the non-planar torsion in the inflationary trajectory – this quantity becomes non-trivial in the second stage of inflation. Finally, we calculate the cosmological observables, which align with Planck data, and discuss potential directions for future research.

¹E-mail: v.basiouris@uoi.gr

²E-mail: dibyac@physics.iitm.ac.in

Contents

| | | |
|----------|---|-----------|
| 1 | Introduction | 1 |
| 2 | Towards moduli stabilization with perturbative effects | 4 |
| 2.1 | The geometrical setup | 5 |
| 2.2 | The effective scalar potential and its stabilization | 6 |
| 3 | Basic idea of multi-field inflation | 13 |
| 3.1 | Kinematic basis decomposition | 14 |
| 3.2 | Multi-field perturbations | 16 |
| 4 | Three-field analysis | 17 |
| 4.1 | Cosmological evolution | 18 |
| 4.2 | Cosmological parameters | 22 |
| 5 | Conclusions | 25 |

1 Introduction

Cosmic inflation refers to a rapid expansion of spacetime occurred in the early Universe [1–3], which smoothed out any fluctuations in spacetime, resulting in a homogeneous and isotropic cosmos. Our theoretical understanding of the Universe and its evolution is based on the Λ CDM model, a six-parameter framework that provides a remarkably accurate explanation for most of the cosmological phenomena. However, it lacks an explanation for the horizon problem and the observed flatness of our Universe. Inflation can provide an explanation for the above two, besides, it can also give rise to the seed for the structure formation we observe today. In addition, observations such as Planck [4] are fully consistent with the simplest inflationary scenario being the leading mechanism to account for the observed anisotropies in the Cosmic Microwave Background (CMB) radiation. Specifically, they align with two strong predictions of inflation: a nearly scale-invariant power spectrum of density perturbations and a stochastic background of gravitational waves.

According to the simplest inflationary scenario, inflation is driven by a scalar field minimally coupled to gravity, whose potential energy dominates over its kinetic energy, causing it to slowly roll over its potential. Once the kinetic energy begins to dominate, inflation comes to an end, providing sufficient spacetime expansion—measured by a parameter called e -folds to resolve the horizon problem. Hence, for inflation to come to a stop eventually, we require a quasi de Sitter accelerated expansion. However, recently proposed consistency conjectures [5–8] imposed on the 4D effective field theory (EFT) derived from a quantum theory of gravity, strongly disfavors vanilla single field inflation. Although, it was hinted

upon in [9] that multi-field inflation with non-trivial field space metric might be able to alleviate this tension.

Moreover, in this decade and the next, various experiments are being launched with aim of detecting the B-mode polarisation in the CMB induced by primordial gravitational waves. They are: CMB-S4 experiment [10], CLASS [11], LiteBIRD [12], and the Simon Observatory [13]. Moreover, upcoming Large Scale Structure surveys, including DESI [14], LSST [15], Euclid [16], and SKA [17], may also detect primordial non-Gaussianities, that may unravel potential interactions during the inflationary era [18]. Both from theoretical and experimental point of view, it thus becomes essential to go beyond the single field vanilla scenario for inflation. In particular, multifield models are generic in supergravity and string theory realisations.

Four-dimensional EFT emerging after dimensional reduction of a superstring theory features various scalar fields, and one/some of them might act as natural candidate/s to drive inflation. This forms the foundation of our three-field inflation model. However, these constructions also have a price to pay; most of the times, the existence of too many scalar fields becomes unavoidable, leading to the so-called cosmological moduli problem (see [19] and the references therein). One also needs to stabilize the scalar field to prevent the appearance of fifth forces. Our aim in this paper is to display a concrete three-field inflationary scenario where the potential energy is constructed from an underlying string theory setup, in particular from a type-IIB flux compactification where the extra dimensions are compactified on a K3 fibred Calabi-Yau (CY). Hence, the first step towards string theory model building is to stabilize the scalar fields. Fortunately, string theory provides sufficient tools (such as Dp branes pierced with magnetized fluxes) to address these issues.

The scalar fields stemming from the closed string sector of type-IIB flux compactifications are of three types: complex-structure (U^i) related to the shapes of the CY, Kähler moduli (T_α) related to the size of the CY, and an Universal scalar field known as axio-dilaton (s) whose vacuum expectation value (vev) determines the string coupling g_s . After dimensional reduction, the scalar potential can be expressed in terms of a holomorphic superpotential and a real Kähler potential. The Type-IIB superpotential depends on the complex structure moduli and dilaton, however it is independent of the Kähler moduli, resulting in the so-called *no-scale structure*. Hence, to stabilize the Kähler moduli, one has to go beyond and add further quantum corrections, such as perturbative corrections to the Kähler potential and non-perturbative effects at the level of superpotential. Note that, the complex-structure and axio-dilaton are usually stabilized at tree-level in presence of fluxes and integrated out.

The most notable candidate models, considering the non-perturbative nature of corrections, are the KKLT [20–29] model and the Large Volume Scenario (LVS) [30–33]. Both type of models address stabilization of the Kähler moduli in type IIB flux compactification despite being flat direction at tree-level. The former utilises non-perturbative effects to be added in a holomorphic superpotential of the Gukov-Vafa-Witten form. The latter addresses the moduli stabilization by a careful interplay between perturbative effects at the level of real Kähler potential and non-perturbative effects to the superpotential. These balance helps to achieve an exponentially large volume of the underlying 6D Calabi-Yau

manifold spanned by the Kähler moduli.

KKLT and LVS being the main two aspects to address full moduli stabilization, recently another class of string vacua also emerged [34–38] where it was shown that large volume can be achieved even without the need of non-perturbative effects as well as to provide an alternative explanation to the long standing problem of Dine-Seiberg [39]– this type of construction is known as pLVS. It is well known that non-perturbative effects are very restrictive and very specific towards the underlying CY geometry, addition of them may lead to satisfying several constraints [40]. Therefore, if a construction ensures a large internal volume without relying on these effects, it becomes much more well-motivated. A recent study [41] provided a more detailed analysis of moduli stabilization and the potential for inflation within this pLVS framework. It also examined the robustness of pLVS against various subleading corrections, including leading-order corrections in inverse string tension, higher-derivative corrections, log-loop corrections from intersecting space-filling $D7$ brane stacks, D-term effects, and Kaluza-Klein as well as winding-type loop corrections.

Supported by these facts, the present work studies the quantum loop corrections in the context of fibre inflation like models [42–44], which are promising for describing inflation. Their advantages have to do with the fact that they include a larger number of cycles $h^{1,1} > 3$ allowing for non-trivial $D7$ branes fluxes to introduce chiral matter to the model. Moreover, fibre inflationary paradigm can be identified as a solution to the η problem in inflation, upgrading the fibre inflation models as ideal candidate to study the expansion of spacetime. In this lore, we are going to present a stabilization scheme, without introducing any non-perturbative effects, where the log-loop corrections together with higher derivative corrections are sufficient to stabilize the "Swiss-cheese" like Calabi-Yau. Furthermore, we explicitly compute on the transformation between the moduli and the canonically-normalized fields, where approximated solutions are found and consistency bounds for the free parameters of the theory are imposed.

Similar to studying any model of inflation, we aim to start by laying the framework to derive the scalar potential in terms of the Kähler moduli. Due to the presence of three-fields, we also discuss the non-planar trajectories and their implications. The effective expansion of spacetime occurs in two stages: initially along the steep direction of the potential, followed by expansion along the remaining two directions as the fields move toward their minima. Note that, throughout inflation all the three fields are active, but their velocity changes while swiftly transitioning between these two stages. In the later phase, the field that fell into the ridge moves relatively slowly, whereas, in the earlier stage, the other two fields move slowly. Since the fields are canonical, the non-planar motion and deviation from a geodesic occur only when the field temporarily falls into a ridge and oscillates there. Finally, we discuss the inflationary predictions and conclude the possible outlook.

The layout of the paper is as follows: in section 2, we present a short overview of the quantum corrections to be added in the Kähler potential along with their string origin and their effect in the stabilization of the Kähler moduli. We end the section by displaying several examples of de Sitter vacua. In section 3, we introduce the multi-field setup where we introduce several concepts like turning rate and torsion. We also discuss their implications at the level of linear perturbation theory. Section 4 mainly covers our detailed

three-field inflationary analysis. After performing several consistency checks stemming from supergravity and the hierarchy of mass scales, we move on to checking the inflationary predictions dubbed in the value of spectral index, spectral tilt, and the amplitude of power spectrum. We also discuss how turning and torsion can affect them. We conclude with our future directions in 5.

2 Towards moduli stabilization with perturbative effects

The perturbative string loop corrections has been recently highlighted in [35] due to their major role in the moduli stabilization mechanism without the need for a non-perturbative effects like the vanilla Large Volume Scenario [42]. In this section, we start by summarizing the world-sheet corrections which are proportional to the Euler characteristic χ of the compactification, followed by an analysis of the origin of string loop corrections within the geometric framework of $D7$ branes in type IIB string theory. After presenting a detailed derivation of the scalar potential, we will showcase several examples of dS vacua where the correct mass hierarchy remains preserved, along with the underlying supergravity approximations.

α^3 corrections

α^3 corrections [45] are added at the level of the Kähler potential to stabilize the volume modulus \mathcal{V} . It acts as an additive factor to the tree-level Kähler potential, giving us:

$$\mathcal{K} = -2 \log \left(\mathcal{V} + \frac{\xi}{2g_s^{3/2}} \right). \quad (2.1)$$

This constant shift ξ of the volume is given in terms of the Euler characteristic of the manifold as:

$$\xi = -\frac{\hat{\xi}(3)}{4(2\pi)^3} \chi. \quad (2.2)$$

Log-loop corrections

Now, the origin of string loop corrections can be traced back to higher derivative terms proportional to R^4 that appearing in the effective action due to multi-graviton scattering of the ten dimensional theory. To make the discussion more precise, we can express the effective action as [34]:

$$\mathcal{S}_{\text{grav}} = \frac{1}{(2\pi)^7 \alpha'^4} \int_{M_4 \times \mathcal{X}_6} e^{-2\phi} \mathcal{R}_{(10)} - \frac{\chi}{(2\pi)^4 \alpha'^4} \int_{M_4} \left(-2\hat{\xi}(3)e^{-2\phi} \pm 4\hat{\xi}(2) \right) R_{(4)}, \quad (2.3)$$

where ϕ is the string dilaton and $R_{(4)}$ denotes the Ricci scalar. in four dimensions and the \pm signs refers to the different type of string theory, type IIA/B theory respectively [46–48]. In the last step, χ is defined as :

$$\chi = \frac{3}{4\pi^3} \int_{\mathcal{X}_6} R \wedge R \wedge R. \quad (2.4)$$

From the above, it is observed that an additional localized Einstein-Hilbert (EH) is induced in four dimensions with a coefficient proportional to χ . These terms correspond to localized gravity vertices in the bulk (in particular at points where $\chi \neq 0$), where their effect is to emit Kaluza-Klein states and gravitons. We assume a background with three intersecting $D7$ branes, where we expect interactions between the closed string modes and KK states in the bulk space. These interactions exhibit in general a logarithmic behavior in the large volume limit transverse to the $D7$ -branes. The new contributions to the R^4 term which are going to be moduli dependent, can be summarized by the following formula [36]:

$$\delta = \frac{4\zeta(2)}{(2\pi)^3} \chi \int_{M_4} \left(1 - \sum_k e^{2\phi} T_k \ln(R_\perp^k / \mathfrak{w}) \right) R_{(4)} . \quad (2.5)$$

T_k is the tension of a $D7$ -brane, and R_\perp stands for the size of the two-dimensional world volume in each brane. Moreover, \mathfrak{w} parametrizes a ‘width’ utilized as an ultraviolet cutoff for the graviton KK modes.

The low-energy dynamics of the four-dimensional effective supergravity theory, emerging from type IIB superstring compactifications on CY orientifolds, can be described by a holomorphic superpotential (W) and a real Kähler potential (K). The tree-level superpotential and Kähler potential are functions of various chiral coordinates. These chiral coordinates are constructed by writing them as a combination of a modulus with a set of RR axions, such as:

$$U^i = v^i - iu^i, \quad s = c_0 + ie^{-\phi}, \quad T_\alpha = c_\alpha - i\tau_\alpha, \quad (2.6)$$

where ϕ is the universal modulus known as dilaton, related to string coupling as $g_s = e^{\langle\phi\rangle}$; u^i is the saxion and v^i is the axion of the complex-structure modulus, and τ_α ’s are the Einstein frame four-cycle volume moduli defined as, $\tau_\alpha = \partial_{t^\alpha} \mathcal{V}$, \mathcal{V} is the overall volume of the Calabi-Yau manifold expressed as $\mathcal{V} = \frac{1}{3!} \kappa_{\alpha\beta\gamma} t^\alpha t^\beta t^\gamma$. Finally, c_0 and c_α ’s are the universal RR axion and RR four-form axions, respectively.

The addition of these corrections changes the tree-level Kähler potential to:

$$K = -\log(-i(s - \bar{s})) - 2 \log \left[\mathcal{V} + \frac{\xi}{2} \left(\frac{s - \bar{s}}{2i} \right)^{3/2} + \left(\frac{s - \bar{s}}{2i} \right)^{-1/2} \delta \right], \quad \delta = \hat{\eta} \log[\tau_i], \quad (2.7)$$

2.1 The geometrical setup

Taking into account the above discussions, we now turn to the derivation of the scalar potential. Fibre inflation model, proposed more than a decade ago in [42] are promising with respect to the embedding of inflation in string compactifications, since they provide a natural solution to the η -problem [49]. Different variations of fibre inflation models have been proposed, where combinations of string loop corrections, Kaluza-Klein and winding loops are considered, leading into inflationary potentials with a sufficient plateau-like form.

In all of these models, the presence of non-perturbative effects to stabilize the blow-up model and the overall volume were common. Recently, another aspect of fibre inflation is also proposed where the interplay of perturbative corrections assured a large volume [50] as

well as full moduli stabilization. The absence of non-perturbative effects eliminates the need for an exceptional del Pezzo divisor. The novelty of this setup is that the usual drawback of fibre inflation where the field space excursion was bounded by Kähler cone conditions were alleviated. In this paper, we follow a similar approach as [50] but consider a different form of the volume, resembling that of K3-fibred Calabi-Yau models like fibre inflation. However, as will become clear in the following subsections, our inflationary predictions deviate significantly from those of the fiber model. To proceed in our analysis, the compactified space volume is given by:

$$\mathcal{V} = f_{3/2}(\tau_i) - \sum_j^{N_{rg}} \lambda_j \tau_j^{3/2} \quad i = 1, \dots, N, \quad (2.8)$$

where the $f_{3/2}$ is a homogeneous function of the Kähler moduli. Despite lacking a complete global embedding for our approach, we are going to adapt the following volume form:

$$\mathcal{V} = \frac{1}{\sqrt{2\alpha}} \sqrt{\tau_7 \tau_6} - \frac{1}{3} \tau_1^{3/2}, \quad (2.9)$$

where α is a model dependent parameter, parametrizing the D-term constraint. Given this form, we cannot a priori characterize the hierarchy between the moduli since the log-loop corrections might affect the anticipated result for $\tau_1 \ll \tau_{6,7}$. Nevertheless, we are obliged to respect the requirement of having a large volume. It would be worth searching through the Kreuzer-Skarke list of Calabi-Yau manifolds embedded in toric varieties [51, 52] for some representative examples where our geometric configuration of intersection $D7$ could lead to large log-loop corrections. τ_1 is the blow-up mode, τ_7 is the usual fibre modulus — the volume of the K3 manifold, and τ_6 is the volume of the \mathbb{P}^2 base. Their cumulative effect ensures that the model remains within the large volume scenario during inflation by adjusting their values.

2.2 The effective scalar potential and its stabilization

Having this volume-form as a starting point, our analysis will be focused on the addition of BBHL term and logarithmic corrections in the Kähler potential without considering any non-perturbative corrections. The large volume in this model is ensured by a cumulative effect of all the perturbative corrections. The Kähler potential upon the insertion of the these corrections can be written as:

$$\mathcal{K} = -\log \left[\frac{s - \bar{s}}{i} \right] - 2 \log \left[\mathcal{V} + \frac{\xi}{2} \left(\frac{s - \bar{s}}{2i} \right)^{3/2} + \left(\frac{s - \bar{s}}{2i} \right)^{-1/2} \sum_i \hat{\eta}_i \log(\tau_i) \right] \quad (2.10)$$

where τ_i stand for the four-cycle moduli, related to the volume of the CY as $\mathcal{V} \sim \tau^{3/2}$, ξ denotes the α' correction-term and the logarithmic corrections $\sim \hat{\eta} \log(\dots)$ are induced along each four-cycle volume moduli. One important last observation we have to make is the fact that the stabilization will completely depend on perturbative corrections. The non-perturbative corrections, which will impose stringent limitation in our construction, could be prevented by considering certain world-volume fluxes that lift fermionic zero modes leading

to zero contribution from these corrections [53–56]. Taking this into account, in this work, we will explore the case where τ_1 no longer remains at small values, but it is stabilized to large values but never taking us away from the domain of large volume. Despite the fact that this approach diverges from the typical paradigm of fibred models, our proposal focuses on the implications on the logarithmic correction on the geometries like (2.9).

Regarding the complex structure moduli z_i as well as the axion-dilaton, they are stabilized at high energies by the supersymmetric flatness conditions:

$$D_{U_i}W = 0 = D_{\bar{U}_i}\bar{W}, \quad D_sW = 0 = D_{\bar{s}}\bar{W} . \quad (2.11)$$

This novel procedure results into one flat direction that appears at the F-term potential level as a consequence of the higher order terms scaling as $\mathcal{O}(1/\mathcal{V}^4)$. Since the scalar potential is parametrized by the three moduli (τ_1, τ_7, τ_6) , we would like to trade one of them in order to introduce the volume \mathcal{V} in the computations. This reparametrization helps us to perform the large volume expansion. So, in order to include the overall volume in our computations, we solve the equation (2.9) with respect to one modulus e.g. τ_6 ,

$$\tau_6 = \frac{\sqrt{2\alpha} \left(\tau_1^{3/2} + 3\mathcal{V} \right)}{3\sqrt{\tau_7}} . \quad (2.12)$$

Using the above definition, we are going to present the necessary computations needed to define the effective F-term scalar potential. Moreover, following [38], the functions in the Kähler potential can be written as follows:

$$Y = \mathcal{V} + \frac{\hat{\xi}}{2} + \hat{\eta} \log \left(\frac{2\alpha\tau_7}{9} \left(\tau_1^{5/2} + 3\mathcal{V}\tau_1 \right)^2 \right) . \quad (2.13)$$

where we have used the fact that the axio-dilaton s and the free parameters of the model $(\hat{\xi}, \hat{\eta})$ are recasted as:

$$s = c_0 + ie^{-\phi}, \quad d = e^{-\phi} \Rightarrow \hat{\xi} = \xi d^{3/2}, \quad \hat{\eta} = \eta d^{-1/2}, \quad d = \frac{1}{g_s} . \quad (2.14)$$

Imposing these redefinitions in (2.13), the Kähler potential can be rewritten as:

$$\mathcal{K} = -\log \left[\frac{s - \bar{s}}{i} \right] - 2 \log [Y] . \quad (2.15)$$

The scalar potential can be computed by the $\mathcal{N} = 1$ supergravity formula:

$$e^{-\mathcal{K}}V_k = K^{A\bar{B}}(D_A W)(D_{\bar{B}}\bar{W}) - 3|W|^2, \quad W = \mathcal{W}_0 . \quad (2.16)$$

The first term of the scalar potential (2.16) will be displayed below, where we expand in terms of $\mathcal{O}(\hat{\eta}, \hat{\xi}/\mathcal{V})$ keeping only the first order terms:

$$K^{A\bar{B}}(D_A W)(D_{\bar{B}}\bar{W}) = 3g_s\mathcal{W}_0^2 \left(1 + \frac{\hat{\xi} - 16\hat{\eta} + \hat{\eta}w}{4\mathcal{V}} + \frac{\hat{\xi}\hat{\eta}(1 - 2w)}{2\mathcal{V}^2} \right) + \mathcal{O} \left(\frac{\hat{\xi}}{\mathcal{V}^n} \right), \quad (2.17)$$

where we define $w = \log\left(\frac{2\alpha\tau_7}{9}(3\mathcal{V}\tau_1 + \tau_1^{5/2})^2\right)$. It is obvious that the second term in (2.16) cancels the first term above, and by turning off $\hat{\eta} \rightarrow 0$, it results to:

$$e^{-\kappa}V_{eff} = \frac{3g_s\mathcal{W}_0^2\hat{\xi}}{4\mathcal{V}} + \mathcal{O}\left(\frac{\hat{\xi}}{\mathcal{V}^n}\right). \quad (2.18)$$

Based on the above, the effective scalar potential can be easily derived and it is shown below:

$$V_{eff} = \frac{3g_s\mathcal{W}_0^2(\hat{\xi} - 16\hat{\eta} + \hat{\eta}w)}{4\mathcal{V}^3} + \mathcal{O}\left(\frac{\hat{\xi}}{\mathcal{V}^n}, \hat{\eta}^n\right). \quad (2.19)$$

As discussed in [42, 44], it is a unique feature of these models to preserve one flat direction. In [42, 44], their approach is to stabilize first the internal volume and the blow-up divisor with an interplay of perturbative and non-perturbative effects, while the τ_7 remains flat. Our approach differs from the aforementioned due to the fact that the logarithmic corrections will be made sufficient to perform the stabilization while keeping track of the remaining flat direction. The previous studies of this kind of approach requires only keeping terms that scales as $\sim \frac{1}{\mathcal{V}^3}$, but now we will prove that even terms proportional to $\sim \frac{\hat{\eta}\hat{\xi}}{\mathcal{V}^4}$ could be significant. Firstly by inspecting the effective potential (2.19), we stabilize with respect to \mathcal{V} while considering $\mathcal{V} \gg \tau_1$:

$$\begin{aligned} \partial_{\mathcal{V}}V_{eff} &= \frac{9\mathcal{W}_0^2g_s}{4\mathcal{V}^4} \left(-\hat{\eta} \log\left(\frac{2\alpha\tau_7}{9}\right) - \hat{\xi} + 2\hat{\eta} \left(\frac{\mathcal{V}}{\tau_1^{3/2} + 3\mathcal{V}} + 8 \right) - 2\hat{\eta} \log\left(\tau_1^{5/2} + 3\tau_1\mathcal{V}\right) \right) = 0, \\ \Rightarrow \mathcal{V} &\cong \frac{e^{\frac{1}{6}(-3\log(\frac{2\alpha\tau_7}{9}) - \frac{3\hat{\xi}}{\hat{\eta}} + 50)} - \tau_1^{5/2}}{3\tau_1}. \end{aligned} \quad (2.20)$$

By substituting the above minimum in the scalar potential, the result is:

$$V_{eff}|_{\mathcal{V}_{min}} = -\frac{27\sqrt{2}\hat{\eta}\tau_1^3\mathcal{W}_0^2(\alpha\tau_7)^{3/2}e^{\frac{3\hat{\xi}}{2\hat{\eta}}}g_s}{\left(\sqrt{2}\sqrt{\alpha\tau_1^5\tau_7}e^{\frac{\hat{\xi}}{2\hat{\eta}}} - 3e^{25/3}\right)^3}, \quad (2.21)$$

where we can see that $\tau_{1,7}$ directions still remain flat. To remedy this, we now include next to leading order term:

$$V_{eff} = \frac{3g_s\mathcal{W}_0^2(\hat{\xi} - 16\hat{\eta} + \hat{\eta}w)}{4\mathcal{V}^3} - \frac{3g_s\mathcal{W}_0^2\hat{\eta}\hat{\xi}(w)}{\mathcal{V}^4} + \mathcal{O}\left(\frac{\hat{\xi}^n}{\mathcal{V}^n}, \hat{\eta}^n\right). \quad (2.22)$$

This new correction will not modify the minimum w.r.t. the volume (at least to a degree that would lead to destabilization), since it is suppressed by $\sim \frac{1}{\mathcal{V}^4}$. Nevertheless, it would slightly lift the contributions to the transverse directions unraveling the importance of quantum corrections to the stabilization of the flat direction. So, the effective potential at \mathcal{V}_{min} is:

$$V_{eff}|_{\mathcal{V}_{min}} = \frac{27\tau_1^4\mathcal{W}_0^2g_s \left(\frac{3\sqrt{2}\hat{\eta}e^{\frac{25}{3} - \frac{\hat{\xi}}{2\hat{\eta}}}}{\tau_1\sqrt{\alpha\tau_7}} + 12\hat{\xi}(3\hat{\xi} - 50\hat{\eta}) - 2\hat{\eta}\tau_1^{3/2} \right)}{4 \left(e^{\frac{1}{6}(-3\log(\frac{2\alpha\tau_7}{9}) - \frac{3\hat{\xi}}{\hat{\eta}} + 50)} - \tau_1^{5/2} \right)^4}, \quad (2.23)$$

where minimizing with respect to τ_7 , there exist one extremum at:

$$\tau_7 = \frac{9e^{\frac{50}{3} - \frac{\hat{\xi}}{\hat{\eta}}}}{2\alpha \left(12\hat{\xi}\tau_1 + \tau_1^{5/2}\right)^2}. \quad (2.24)$$

Given the above extremum, we achieve a saddle at:

$$V_{eff}|_{\mathcal{V}_{min}}^{\langle\tau_7\rangle} = \frac{3\mathcal{W}_0^2(\hat{\xi} - 16\hat{\eta})g_s}{256\hat{\xi}^3} > 0. \quad (2.25)$$

Despite the fact that the effective potential is positive at the minimum given $\hat{\xi} > 16\hat{\eta}$, not all the directions are stabilized. As we can see in (2.24), the extremum along τ_7 depends on τ_1 which is yet to be fixed. Thus, we are obliged to investigate the possibility of additional corrections, whose effects could achieve this. The following correction can also be induced as an addition to the leading order α'^3 corrections. They are summarized in the following contributions:

Higher-derivative string corrections: They appear at the level of α'^3 corrections multiplying an F^4 term and they modify the 4D EFT scalar potential as [57]:

$$V_{F^4} = -k^2 \frac{|\lambda|\mathcal{W}_0^4}{g_s^{3/2}\mathcal{V}^4} \Pi_i t^i, \quad (2.26)$$

where Π_i is a topological number depending on the intersection of the divisors and λ is unknown combinatorial factor.

Inflationary potential and moduli stabilization

In the present model, we are going to utilize this subleading correction and study their implications both on the stabilization procedure and on the inflationary analysis:

$$V_{eff} = \frac{3g_s\mathcal{W}_0^2(\hat{\xi} - 16\hat{\eta} + \hat{\eta}w)}{4\mathcal{V}^3} - \frac{3g_s\mathcal{W}_0^2\hat{\eta}\hat{\xi}(w)}{\mathcal{V}^4} + \frac{c}{\mathcal{V}^4}(t_1 + t_6 + t_7) + V_{up} + \mathcal{O}\left(\frac{1}{\mathcal{V}^5}\right), \quad (2.27)$$

where the c parameter quantifies the overall factor of F^4 corrections depending on the string coupling g_s and the fluxes \mathcal{W}_0 . In addition, we have added a small constant V_{up} which will be used to obtain an almost Minkowski/dS vacuum. Some efforts towards carefully computing this uplifting term have been analyzed in [43, 58]. Now, for concreteness, we should stress the fact that winding loop corrections and KK corrections should also be considered in a concrete model as have been stressed in [41, 50], but since we are agnostic about the value of their coefficients, in the current work we only study the case where only F^4 corrections is enough to stabilize the flat directions and produce a dS-shallow potential.

The relation between the two-cycle moduli and the four-cycle moduli is summarized below and it can be used to express the F^4 correction:

$$t_1 = \sqrt{\tau_1}, \quad t_7 = \frac{1}{\sqrt{2\alpha}} \frac{\tau_6}{\sqrt{\tau_7}}, \quad t_6 = \frac{1}{\sqrt{2\alpha}} \sqrt{\tau_7}. \quad (2.28)$$

$$V_{F^4} = \frac{c}{\mathcal{V}^4} \left(\frac{\sqrt{\tau_7}}{\sqrt{2}\sqrt{\alpha}} + \sqrt{\tau_1} + \frac{\tau_1^{3/2} + 3\mathcal{V}}{3\tau_7} \right), \quad c = -k^2 \frac{|\lambda| \mathcal{W}_0^4}{g_s^{3/2}} \Pi_i. \quad (2.29)$$

Based on this addition, one can proof that the flat direction along $\{\tau_1, \tau_7\}$ are lifted. In order to connect this section with the inflationary analysis in the next section, it is easier to express the potential in the normalized field basis spanned by $(\varphi_1, \varphi_2, \varphi_3)$. To do so, we need to write down the leading order terms of the Kähler metric, which are:

$$K_{ij} = \begin{pmatrix} \frac{1}{4\tau_7^2} & 0 & 0 \\ 0 & \frac{1}{2\tau_6^2} & 0 \\ 0 & 0 & \frac{\sqrt{\alpha\tau_7}}{4\sqrt{2}\sqrt{\tau_1}\tau_6\tau_7} \end{pmatrix}. \quad (2.30)$$

Given the above form, the kinetic term are now written as:

$$K_{ij} \partial T_i \partial \bar{T}_j = \sum_i \frac{\partial T_i \partial \bar{T}_i}{(T_i + \bar{T}_i)^2} = \sum_i \frac{1}{2} (\partial \varphi_i)^2 + \dots. \quad (2.31)$$

The new relation between the old and new bases are the following:

$$\tau_7 = e^{\sqrt{2}\varphi_1}, \quad \tau_6 = e^{\varphi_2}, \quad (2.32)$$

$$\tau_1 = \left(\frac{3^4 \varphi_3^4 e^{(\sqrt{2}\varphi_1 + 2\varphi_2)}}{2^5 \alpha} \right)^{1/3}, \quad \mathcal{V} = \frac{(4 - 3\varphi_3^2) e^{\frac{\varphi_1}{\sqrt{2}} + \varphi_2}}{4\sqrt{2}\sqrt{\alpha}}. \quad (2.33)$$

Finally, we display the scalar potential in the new basis as:

$$\begin{aligned} V_{eff} = V_{up} & - \frac{1024\alpha^2 \hat{\xi} \hat{\eta} g_s \mathcal{W}_0^2 e^{-2\sqrt{2}\varphi_1 - 4\varphi_2} \left(\log \left(\frac{9^4 \varphi_3^8}{2^{10} \alpha^2} \right) + 8\sqrt{2}\varphi_1 + 10\varphi_2 \right)}{(4 - 3\varphi_3^2)^4} \\ & - \frac{32\sqrt{2}\alpha^{3/2} g_s \mathcal{W}_0^2 e^{-\frac{3\varphi_1}{\sqrt{2}} - 3\varphi_2} \left(\hat{\eta} \left(\log \left(\frac{9^4 \varphi_3^8}{2^{10} \alpha^2} \right) + 8\sqrt{2}\varphi_1 + 10\varphi_2 - 48 \right) + 3\hat{\xi} \right)}{(3\varphi_3^2 - 4)^3} \\ & + \frac{512 \cdot 2^{1/6} \alpha^{3/2} c e^{-\frac{5\varphi_1}{\sqrt{2}} - 4\varphi_2} \left((9\alpha \varphi_3^2 e^{2\sqrt{2}\varphi_1 + \varphi_2})^{1/3} + 2^{1/3} (e^{\sqrt{2}\varphi_1} + e^{\varphi_2}) \right)}{(4 - 3\varphi_3^2)^4}. \quad (2.34) \end{aligned}$$

Note that, the potential carries an asymptote along the φ_3 direction at $\varphi_3 = \sqrt{4/3}$. The implications of this will have a clear effect on the inflationary analysis as will be shown in section 4.

Due to the complexity of the above potential, we can reduce its form by considering an expansion with respect to a small parameter y . One can readily see in the above form, that there is a factor of $4 - 3\varphi_3^2$, which can be recasted to:

$$\varphi_3^2 = \frac{y + 4}{3}. \quad (2.35)$$

Given the definitions in (2.33), we can see that ϕ_3 is bounded, since we want a positive volume. One can deduce from that the y parameter has to be small in order to satisfy the

above constrain. So, we can perform a an expansion with respect to this parameter. The leading order terms of this expansion results into:

$$\begin{aligned}
V_{eff}^{appr} = & \frac{32 \alpha^{3/2} e^{-\frac{5\varphi_1}{\sqrt{2}} - 4\varphi_2}}{3y^4} \left[48\sqrt{2}c \left(e^{\sqrt{2}\varphi_1} + e^{\varphi_2} \right) + 4 \times 2^{5/6} (3\alpha)^{1/3} c(y+12) e^{\frac{1}{3}(2\sqrt{2}\varphi_1 + \varphi_2)} \right. \\
& - 3W_0^2 y g_s e^{\sqrt{2}\varphi_1 + \varphi_2} \left(2\hat{\eta} \left(\sqrt{2}(-\log(2\alpha) + 5\varphi_2 - 24) + 8\varphi_1 \right) + 3\sqrt{2}\hat{\xi} \right) \\
& \left. - 96\sqrt{\alpha} \hat{\xi} \hat{\eta} e^{\frac{\varphi_1}{\sqrt{2}}} W_0^2 g_s \left(-2\log(2\alpha) + 8\sqrt{2}\varphi_1 + 10\varphi_2 + y \right) \right] + V_{up} . \quad (2.36)
\end{aligned}$$

We could further simplify our formula considering the regime where the α parameter is small $\alpha \ll 1$. The simpler formula for the effective potential is then given by:

$$\begin{aligned}
V_{eff}^{appr} = & \frac{32\alpha^{3/2} e^{-\frac{5\varphi_1}{\sqrt{2}} - 4\varphi_2}}{3y^4} \left[4\sqrt{2}c \left(12 \left(e^{\sqrt{2}\varphi_1} + e^{\varphi_2} \right) + (y+12)(6\alpha e^{(2\sqrt{2}\varphi_1 + \varphi_2)})^{1/3} \right) - \right. \\
& \left. - W_0^2 y g_s e^{\sqrt{2}\varphi_1 + \varphi_2} \left(-\sqrt{2}\hat{\eta} \log(64\alpha^6) + 9\sqrt{2}\hat{\xi} + 6\hat{\eta} \left(8\varphi_1 + \sqrt{2}(5\varphi_2 - 24) \right) \right) \right] + V_{up} . \quad (2.37)
\end{aligned}$$

From this expression, one can easily minimize the potential with respect to the variable y . This can be approximated as:

$$y \cong \frac{64\sqrt{2}c e^{-\sqrt{2}\varphi_1 - \varphi_2} \left((6\alpha e^{(2\sqrt{2}\varphi_1 + \varphi_2)})^{1/3} + e^{\sqrt{2}\varphi_1} + e^{\varphi_2} \right)}{W_0^2 g_s \left(\sqrt{2}\hat{\eta}(-\log(64\alpha^6) + 30\varphi_2 - 144) + 9\sqrt{2}\hat{\xi} + 48\hat{\eta}\varphi_1 \right)} . \quad (2.38)$$

By recalling the redefinition in (2.35), the minimum along φ_3 direction is determined as:

$$\varphi_{3,min}^2 = \frac{1}{3}(y+4) . \quad (2.39)$$

As for the other two perpendicular directions, we could substitute the minimal value of y in the effective scalar potential of equation (2.37), which leads to the following minima along (φ_1, φ_2) :

$$\varphi_{2,min} \cong \frac{1}{30} \left(\log(64\alpha^6) - \frac{9\hat{\xi}}{\hat{\eta}} - 24\sqrt{2}\varphi_1 + 30 W_{0/-1} \left(\frac{2^{9/5} e^{\frac{1}{30} \left(\frac{9\hat{\xi}}{\hat{\eta}} + 54\sqrt{2}\varphi_1 - 184 \right)}}{3\alpha^{1/5}} \right) + 184 \right) , \quad (2.40)$$

$$\varphi_{1,min} \cong \frac{6\hat{\eta} \log(\alpha) - 9\hat{\xi} + 2\hat{\eta} \left(144 + 15 \log\left(\frac{13}{5}\right) + \log(8) \right)}{54\sqrt{2}\hat{\eta}} . \quad (2.41)$$

To prove the validity of our approximate formula of the potential in (2.37) and the exact potential in (2.34), we are going to sketch the potentials in the vicinity of the global minimum.

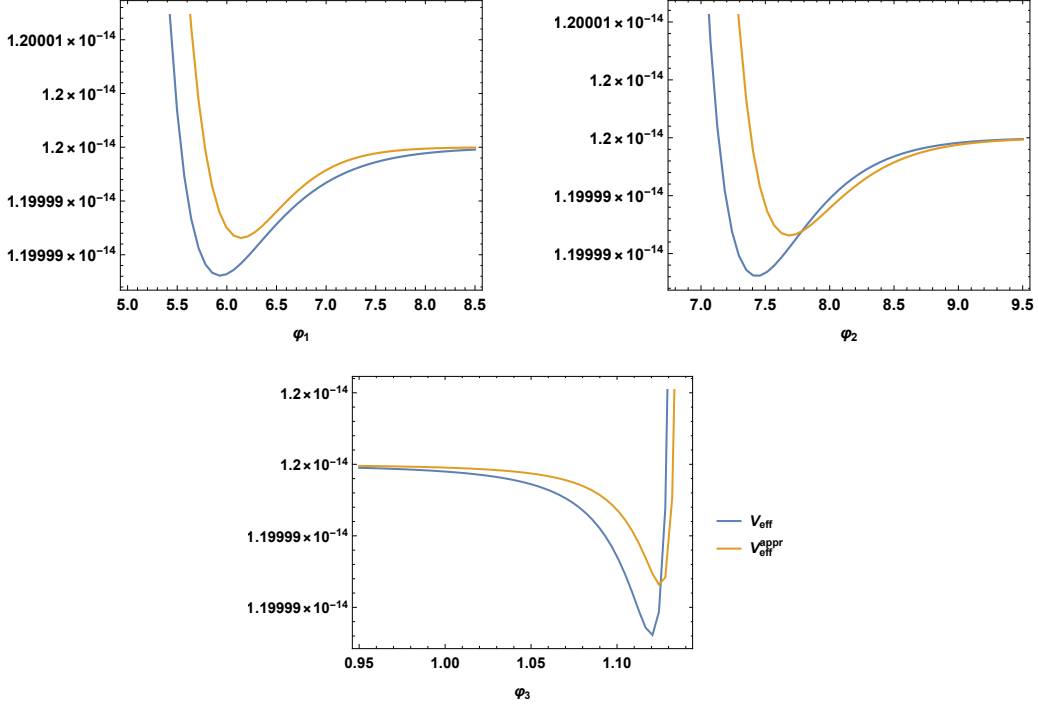


Figure 1: Comparison between analytical and numerical computation of minimum along φ_1, φ_2 and φ_3 directions. The parameters used in these plots correspond to Model 1 of Table 2.

It is readily seen that our approximated and numerical solutions match modulo tiny departure. Note that, for the inflationary analysis studied in section 4, we work with the potential with the exact form as demonstrated in (2.27).

Mass-scales

Let us now move on to discussing several mass scales associated with the underlying type-IIB flux compactification. The first mass scale of interest is the string scale which for consistency of the low-energy string theory should be much less than the Planck scale with the relation³ $M_s = \frac{g_s^{1/4} \sqrt{\pi}}{\sqrt{\mathcal{V}}} M_{pl}$. Next, we define our Kaluza-Klein scale associated with the bulk *i.e.* $\tau_{\text{bulk}}^{3/2} = \mathcal{V}$, $M_{KK} = \frac{\sqrt{\pi}}{\mathcal{V}^{2/3}} M_{pl}$. Gravitino mass is given by $m_{3/2} = \sqrt{\kappa} \frac{|W_0|}{\mathcal{V}} M_{pl}$. $m_{3/2}$ sets the scale of all complex structure moduli, the dilaton and the Kähler moduli. Another important consistency requirement is $m_{3/2} < M_{KK}$, so that the gravitino mass of the 4d EFT is not integrated out. In order to trust the underlying EFT, we need to maintain the following hierarchy of mass scales,

$$m_{3/2} < M_{KK} < M_s < M_{pl}. \quad (2.42)$$

³Note that, here instead of using natural units, we have reintroduced the Planck scale to understand the hierarchy between various mass scales.

Example dS-vacua

In the following tables, several numerical examples are presented, where the values of the free parameters are displayed along with the values of the moduli/fields at their corresponding minimum.

| | τ_1 | τ_7 | τ_6 | \mathcal{V} | φ_1 | φ_2 | φ_3 |
|---------|--------------------|----------|----------|-----------------|-------------|-------------|-------------|
| Model 1 | 1.35×10^5 | 4403 | 1690 | 1×10^6 | 5.93 | 7.43 | 1.12 |
| Model 2 | 3.56×10^5 | 7120 | 2732 | 2×10^6 | 6.27 | 7.91 | 1.14 |
| Model 3 | 3.79×10^6 | 44636 | 17191 | 1×10^8 | 7.57 | 9.75 | 1.13 |

| | $m_{\langle\varphi_1\rangle}$ | $m_{\langle\varphi_2\rangle}$ | $m_{\langle\varphi_3\rangle}$ | $m_{3/2}$ | M_{KK} | M_s |
|---------|-------------------------------|-------------------------------|-------------------------------|------------------------|-----------------------|-----------------------|
| Model 1 | 3.42×10^{-8} | 4.63×10^{-10} | 2.17×10^{-10} | 5.72×10^{-8} | 1.72×10^{-4} | 1.73×10^{-4} |
| Model 2 | 3.2×10^{-8} | 2.01×10^{-10} | 9.27×10^{-11} | 3.46×10^{-8} | 1.1×10^{-4} | 1.19×10^{-4} |
| Model 3 | 2.32×10^{-11} | 2.28×10^{-13} | 1.05×10^{-13} | 2.87×10^{-10} | 7.72×10^{-6} | 9.51×10^{-6} |

Table 1: Three different numerical solutions for the minima with their corresponding masses.

| | g_s | $ \mathcal{W}_0 $ | $\hat{\xi}$ | $ \hat{\eta} $ | α | $ \lambda $ | V_{up} |
|---------|----------------------|-------------------|-------------|----------------|--------------------|-------------|------------------------|
| Model 1 | 10^{-4} | 30 | 11.5 | 0.5 | 2×10^{-5} | 0.09 | 1.2×10^{-14} |
| Model 2 | 8.5×10^{-5} | 38 | 13.5 | 0.5 | 5×10^{-5} | 0.04 | 2.23×10^{-20} |
| Model 3 | 10^{-5} | 50 | 19.5 | 0.5 | 1×10^{-6} | 0.078 | 2.86×10^{-26} |

Table 2: The free parameters used for the examples presented above.

A very recent study [59] showed that the higher derivative corrections are still under consideration regarding the correct embedding in the supersymmetric field theories and their dimensional reduction. In this work it is argued that the inclusion of all the higher derivative terms derived from the ten dimensional theory, i.e. an extension of the previous study [57], could in principle modify the strength of the F^4 corrections by affecting the values of the λ parameter. Thus, in the case of a constant superpotential, one could argue that the scale of λ parameter is expected to be enhanced $\lambda > \mathcal{O}(10^{-3})$. Our example could be seen as an example of the importance of these F^4 corrections in the moduli stabilization. One more crucial comment that needs to be highlighted is the fact that if the Kähler dependence of the those corrections is changed due to the extended operators, the form of the effective potential drastically changed. We refer for relevant discussion to [59]. In the following section, we continue our discussion on the fundamental concepts necessary for conducting a three-field inflationary analysis.

3 Basic idea of multi-field inflation

The purpose of this section is to set the stage for the three-field inflationary scenario that we are going to present in the next section. We begin by writing the Lagrangian for multiple

scalar fields minimally coupled with gravity in $(3 + 1)$ -dimensional curved spacetime:

$$S = \int d^4x \sqrt{-g} \left[M_{pl}^2 \frac{R_4}{2} - \frac{\mathcal{G}_{ab}}{2} \partial_\mu \phi^a \partial^\mu \phi^b - V(\phi^a) \right], \quad (3.1)$$

where Greek letters label the 4d spacetime indices of Friedman-Lemaitre-Robertson-Walker (FLRW) metric with $(-, +, +, +)$ metric signature. Lower latin indices denote field-space entries with $(a, b \equiv 1, 2, 3)$ and the metric is \mathcal{G}_{ab} . $V(\phi^a)$ is the scalar potential in terms of ϕ^a . $M_{pl}^2 = (8\pi G_N)^{-1}$ is the reduced Planck mass with G_N being the Newton's constant. We will work in natural units, hence from now on we will put $M_{pl} = 1$. In an FLRW spacetime, Einstein's equation of motion for a scalar field known as inflaton, takes the following form,

$$H^2 = \frac{1}{3} \left(\frac{\dot{\phi}^2}{2} + V(\phi^a) \right), \quad (3.2)$$

$$\ddot{\phi}^a + 3H\dot{\phi}^a + \Gamma_{bc}^a \dot{\phi}^b \dot{\phi}^c + \mathcal{G}^{ab} V_b = 0, \quad (3.3)$$

here

$$\dot{\phi}^2 \equiv \mathcal{G}_{ab} \dot{\phi}^a \dot{\phi}^b. \quad (3.4)$$

Note that H is the Hubble parameter overseeing the expansion of the spacetime during inflation and it is related to the scale factor of FLRW metric. The Christoffel symbols in (3.3) is calculated from the field space metric \mathcal{G}_{ab} and V_a is the derivative of the potential with respect to the scalar field ϕ^a . In multi-field inflationary models, (3.2) acts as a constraint and it is enough to solve just the field equations. The equations above are written in physical time but for our purpose of studying inflation, it is more convenient to switch to number of e-folds (N) which is related to time as $dN = H dt$.

Inflation is a nearly exponential evolution of the space-time. This is ensured by requiring the fractional change of the Hubble parameter per e-fold, denoted by $d \ln H / dN$ to be small. In the same spirit, one can define a series of Hubble slow-roll parameters ϵ_i s where $\epsilon_1 = -d \ln H / dN$. ϵ_1 is the first Hubble slow-roll parameter and for brevity we will drop the subscript. In order for inflation to last at least 60 e-folds to, necessary to solve the horizon problem, ϵ should remain small for a sufficient number of Hubble times and this is measured by the second Hubble slow-roll parameter η , defined as:

$$\eta \equiv \frac{\dot{\epsilon}}{\epsilon H} = \frac{\ddot{H}}{H \dot{H}} + 2\epsilon = 2\delta_\phi + 2\epsilon \ll 1, \quad (3.5)$$

where a small η also requires a small δ_ϕ .

3.1 Kinematic basis decomposition

We are interested in a three-field inflation with turning and torsion in field space. Hence, it is natural to work on kinetic basis by decomposing the inflationary trajectory into tangent, normal and a binormal direction as shown in figure 2. An extensive study on three-field inflation called helix-trajectory inflation using an hyperbolic metric is carried out in [60]

and further extended in [61–63]. In this lore, let us introduce unit tangent (T^a), normal (N^a) and binormal (B^a) vectors as following:

$$\begin{aligned}
T^a &= \frac{\dot{\phi}^a}{\dot{\phi}}, & N^a &= \frac{\mathcal{D}_N T^a}{\Omega_1}, & B^a &= \frac{D_N N^a + \Omega_1 T^a}{\tau}, \\
T^a T_a &= B_a B^a = N_a N^a = 1, & N^a T_a &= B^a T_a = N^a B_a = 0, \\
\Omega_1 &= \frac{\Omega}{H}, & \Omega &= |\mathcal{D}_t T|, & \tau B^a &= \mathcal{D}_N N^a + \Omega_1 T^a.
\end{aligned} \tag{3.6}$$

Ω_1 is known as the dimensionless *turning rate*, Ω is dimensionful turning rate and τ denotes the dimensionless *torsion* [61, 64]. Both of them determine how much an inflationary trajectory deviates from a geodesic one ($\mathcal{D}_t T = 0$, $T = \sqrt{\mathcal{G}_{ab} T^a T^b}$). In a three-dimensional field-space (x, y, z) for example, Ω denotes how much the inflationary trajectory is bending in the $x - y$ plane and τ denotes what is its motion along the vertical z -direction. When $\Omega > 0$ the trajectory undergoes turning and when $\tau > 0$ the trajectory is non-planar. If both (Ω, τ) are constant, the trajectory takes a helical path as found in [60]. Note that, the kinematic basis as well as the torsion is not well defined when $\Omega = 0$. In our work however, as presented in section 4, the non-geodesic behavior will be manifested not in their kinetic terms but in the scalar potential through non-trivial coupling of scalar fields. Ω denotes the norm of the unit tangent vector and has one mass dimension. These can be summarised in terms of Frenet-Serret system as follows:

$$\mathcal{D}_N \begin{pmatrix} T^a \\ N^a \\ B^a \end{pmatrix} = \begin{pmatrix} 0 & \Omega_1 & 0 \\ -\Omega_1 & 0 & \tau \\ 0 & -\tau & 0 \end{pmatrix} \begin{pmatrix} T^a \\ N^a \\ B^a \end{pmatrix}. \tag{3.7}$$

With the help of the equation of motion (3.3), the definitions of Ω_1 and τ can be related to the inflationary potential as [62]:

$$\Omega = -\frac{V_N}{H\phi'}, \quad ' = \frac{d}{dN}, \tag{3.8}$$

$$\tau = -\frac{V_{BT}}{\Omega_1 H^2}, \tag{3.9}$$

where $V_N = N^a V_a$, $V_{BT} = V_{ab} T^a B^b$ and $\nabla_a A_b \equiv \partial_a A_b - \Gamma_{ab}^c A_c$, for some vector A_b .

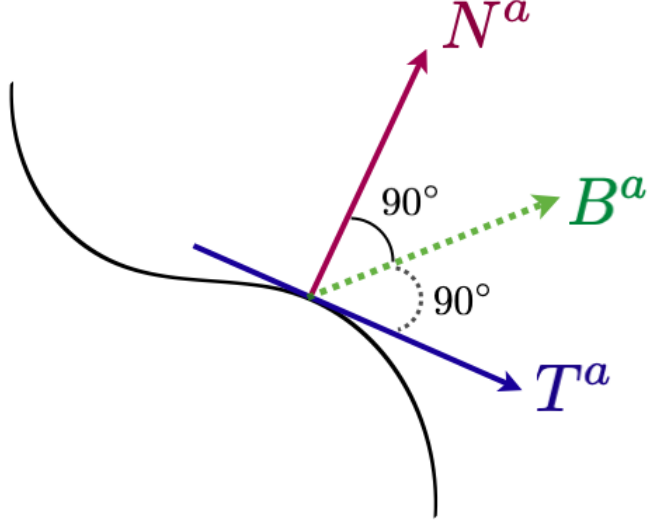


Figure 2: The black line corresponds to the inflationary trajectory on which T^a is an unit vector tangential to it. N^a is another unit vector normal to the trajectory and B^a denotes the unit vector normal to both T^a and N^a .

To study the masses of the scalar fields as well as to study multi-field perturbations, we define two matrices. \mathbb{M}_b^a is the mass-matrix of the scalar fields computed from $V(\phi^a)$ and the projection of the \mathbb{M}_b^a along the directions of the unit vectors is denoted by \mathbb{M} :

$$\mathbb{M}_b^a = \nabla^a \nabla_b V, \quad \mathbb{M} = \begin{pmatrix} V_{TT} & V_{TN} & V_{TB} \\ V_{NT} & V_{NN} & V_{NB} \\ V_{BT} & V_{BN} & V_{BB} \end{pmatrix}, \quad (3.10)$$

where $V_{TT} = T^a T^b \nabla_a \nabla_b V$.

3.2 Multi-field perturbations

In case of multi-field inflation, it is standard to decompose the linear equation of motion for Mukhanov-Sasaki variable in kinematic basis *i.e.* along (T^a, N^a, B^a) . The projection of field fluctuations Q^a along the unit vectors are $Q_i = (Q_T, Q_N, Q_B) \equiv (Q^a T_a, Q^a N_a, Q^a B_a)$. The equations of motion in terms of Q_i are [62–64]:

$$\begin{aligned} \mathcal{D}_N(Q')^i + F_j^i(Q')^j + C_j^i Q^j &= 0, \\ F_j^i &\equiv (3 - \epsilon)\delta_j^i - 2\Omega_j^i, \\ C_j^i &= \left(\frac{k}{aH}\right)^2 \delta_j^i + \begin{pmatrix} 0 & -2(3 - \epsilon)\Omega_1 & 0 \\ 0 & \mathcal{M}_{NN} - \Omega_1^2 - \tau^2 & \mathcal{M}_{NB} - \tau(3 - \epsilon) \\ 0 & \mathcal{M}_{NB} + \tau(3 - \epsilon) & \mathcal{M}_{BB} - \tau^2 \end{pmatrix} + \mathcal{O}(\epsilon^2, \eta, \nu, \nu_\tau). \end{aligned} \quad (3.11)$$

Primes denote a derivative with respect to conformal time $d\tau = dt/a(t)$. We defined $\nu = \Omega'_1/\Omega_1$ and $\nu_\tau = \tau'/\tau$. The mass terms appearing in (3.11) such as $(\mathcal{M}_{NN}, \mathcal{M}_{NB}, \mathcal{M}_{BB})$

can be obtained by contracting \mathcal{M}_{ab} with (N^a, B^a) where \mathcal{M}_{ab} is:

$$\mathcal{M}_{ab} = \frac{V_{ab}}{H^2} - 2\epsilon R_{aTb} + 2\epsilon(3 - \epsilon)T^a T^b + \sqrt{2\epsilon} \frac{T_a V_b + T_b V_a}{H^2} \quad (3.12)$$

In order to further simplify the above set of equations one has to compare between the adiabatic mass and entropic masses. If the entropic masses are larger or comparable to the adiabatic mass, one has to consider the effect of all the fields in the perturbative analysis which thus modify the spectral index and spectral tilt [60] through a parameter called speed of sound c_s . It is the propagation speed of the adiabatic perturbation, expressed in terms of the ratio of entropic masses. The study of perturbation with reduced speed of sound and non-trivial turns is studied for the two-field case in [65–67] and in the three-field scenarios in [68, 69]. On the other hand, for the inflationary analysis done in this paper — the mass gap between the adiabatic and entropic masses are large enough so that we integrate out the latter. In this case, we can study the inflationary perturbation as a quasi-single field effective theory, knowing that it is subject to $M_{TT}/M_{\text{entropic}}$ corrections.

4 Three-field analysis

In this section, we will thoroughly analyze the complete multi-field inflationary evolution and the detailed predictions of the model. To achieve this, we begin by outlining the consistency checkpoints that must be met in a viable string theory model building.

Consistency checks

1. To reside in the semi-classical regime, we need to achieve small g_s and large volume \mathcal{V} . From the examples presented in table (1,2), we can observe that all of them meet the specified criteria with $g_s \sim \mathcal{O}(10^{-4})$ and $\mathcal{V} \sim \mathcal{O}(10^6)$. Due to the same reason, it is easier to trust the underlying EFT in our model by requiring:

$$V_{\alpha'^3} > V_{F^4},$$

which means the leading order BBHL-term proportional to $\hat{\xi}$ in the perturbative expansion in α' should be larger compared to the higher derivative F^4 term, proportional to λ . The above inequality simplifies to:

$$\mathcal{V} > \frac{W_0^2 \lambda}{2\pi^2 \sqrt{g_s} \hat{\xi}}, \quad (4.1)$$

where \mathcal{V} is the volume in (2.9). For a typical set of parameters, one can show that the inequality poses a less strict constraint for the parameter sets presented in this paper. For the inflationary example as well as the models presented in table (1,2), we get $\mathcal{V} > \mathcal{O}(10^2)\lambda$, with $\lambda \ll 1$.

2. High energy stringy effects can be neglected if each four-cycle considered in this work, which are τ_1, τ_6, τ_7 , has volume larger than the string scale⁴: $\text{Vol}_s^{1/4} \gg \sqrt{\alpha'}$. The

⁴For details on how the volumes and 10D metric in Einstein and string frame are related see [70].

string frame and Einstein frame volume is related as: $\text{Vol}_s = g_s \text{Vol}_E = g_s \tau_E l_s$ with $l_s = 2\pi\sqrt{\alpha'}$. We arrive at the following relation:

$$\delta_{\tau_i} \equiv \frac{1}{g_s (2\pi)^4 \tau_i} \ll 1 \quad \forall i. \quad (4.2)$$

From table-1, we see that with $\tau_i \sim \mathcal{O}(10^3 - 10^4)$ and $g_s \sim \mathcal{O}(10^{-4})$, it is straightforward to satisfy this condition.

3. To trust the α' expansion, one has to satisfy: $\delta_\xi = \frac{\hat{\xi}}{2\mathcal{V}} \ll 1$. For $\hat{\xi} \sim \mathcal{O}(10)$ and $\mathcal{V} \sim \mathcal{O}(10^6)$, it is easily satisfied in our models.

4. Again from the consistency of the EFT, throughout the inflationary evolution, we need⁵:

$$m_{\varphi_i} < H < M_{kk}^{\text{bulk}} < M_s < M_{pl}. \quad (4.3)$$

5. Last but not least, the inflationary prediction should be in compliance with the Planck 2018 data [4]:

$$P_s = 2.105 \pm 0.03 \times 10^{-9}, \quad n_s = 0.9649 \pm 0.0042, \quad r < 0.036, \quad (4.4)$$

at a pivot scale of 0.05 Mpc^{-1} .

4.1 Cosmological evolution

We now analyze the three-field cosmological evolution in a fully canonical basis spanned by $(\varphi_1, \varphi_2, \varphi_3)$. The field space metric being flat makes both the Christoffel symbols and the Ricci scalar zero. In this setup, the evolution equations of (3.3), in the canonical basis boils down to these simpler set of equations in number of e-folds:

$$\begin{aligned} \varphi_1'' &= - \left(\frac{1}{2} (\varphi_1'^2 + \varphi_2'^2 + \varphi_3'^2) + 3 \right) \varphi_1' - \frac{V_{,\varphi_1}}{H^2}, \\ \varphi_2'' &= - \left(\frac{1}{2} (\varphi_1'^2 + \varphi_2'^2 + \varphi_3'^2) + 3 \right) \varphi_2' - \frac{V_{,\varphi_2}}{H^2}, \\ \varphi_3'' &= - \left(\frac{1}{2} (\varphi_1'^2 + \varphi_2'^2 + \varphi_3'^2) + 3 \right) \varphi_3' - \frac{V_{,\varphi_3}}{H^2}, \quad ' = \frac{d}{dN}. \end{aligned} \quad (4.5)$$

V is the scalar potential in (2.34) which consists of leading order α'^3 BBHL-term, log-loop corrections, higher derivative F^4 corrections and a constant uplift term resulting to a Minkowski-like vacuum of the potential at its global minimum. We are agnostic about the exact computation of the uplift term, it can either be a D-term uplift [32], a T-brane uplift [72] or an anti-brane uplift [5, 58, 73, 74]. We now present a three-field inflationary model where all the three fields $(\varphi_1, \varphi_2, \varphi_3)$ are displaced from their respective minimum. We get sufficient e-folds as these fields complete their journey towards their minima and oscillate

⁵See [71] for a slightly different hierarchy of scales where the inequalities between inflaton mass m_{inf} and the underlying Hubble scale is interchanged to $m_{\text{inf}} > H$ throughout the slow-roll inflationary evolution in a multi-field scenario.

there to start the reheating process⁶. Below, we discuss one benchmark model which uses the following set of parameters:

| g_s | $ W_0 $ | $ \hat{\eta} $ | α | $\hat{\xi}$ | λ | C_{up} | φ_1^0 | φ_2^0 | φ_3^0 | $\langle\varphi_1\rangle$ | $\langle\varphi_2\rangle$ | $\langle\varphi_3\rangle$ |
|-------|---------|----------------|----------|-------------|-----------|------------------------|---------------|---------------|---------------|---------------------------|---------------------------|---------------------------|
| 0.001 | 38 | 0.5 | 0.0001 | 16 | 0.008 | 2.45×10^{-14} | 4.9 | 10.0 | 1.1 | 7.09 | 9.06 | 1.15437 |

Table 3: Model parameters and initial conditions for inflation labelled by superscript 0.

| $m_{\langle\varphi_1\rangle}^2$ | $m_{\langle\varphi_2\rangle}^2$ | $m_{\langle\varphi_3\rangle}^2$ | M_s/M_{pl} | M_{KK}/M_{pl} | $m_{3/2}/M_{pl}$ | H/M_{pl} |
|---------------------------------|---------------------------------|---------------------------------|-----------------------|-----------------------|----------------------|----------------------------|
| 1.54×10^{-6} | 2.51×10^{-14} | 5.33×10^{-15} | 1.36×10^{-3} | 1.25×10^{-3} | 4.5×10^{-6} | $\sim 6.95 \times 10^{-8}$ |

Table 4: The values of different mass scales relevant to model building are considered. The Hubble parameter, derived from (3.2), remains nearly constant throughout the inflationary evolution, which is why a wiggly sign has been included.

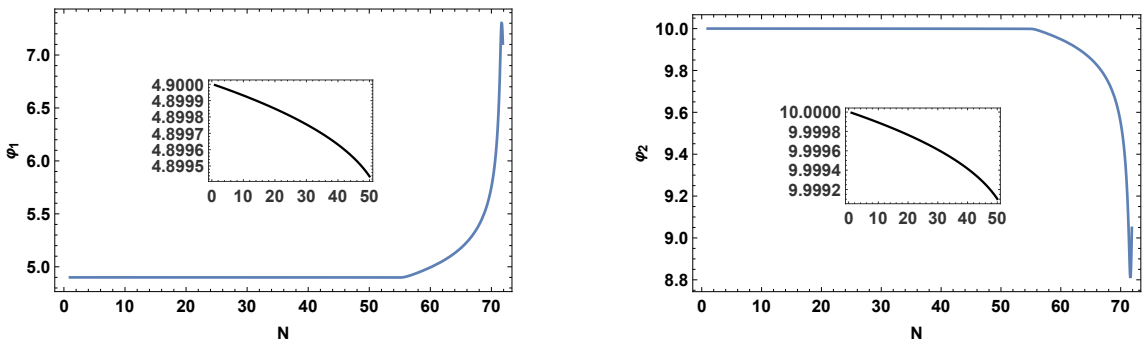
Masses of the inflatons tabulated above are Eigenvalues of the Hessian matrix computed using (2.34) at their respective minimum. In accordance with the consistency checks ((2.42) and (4.3)) stated above, the hierarchy of various mass scales are satisfied *i.e.* :

$$m_{3/2} < M_{KK} < M_s < M_{pl}, \quad \text{and} \quad M_{\varphi_i} \equiv M_{\text{inf}} < H.$$

For this benchmark model, the overall volume of (2.9) is $\mathcal{V} \sim \mathcal{O}(10^4)$. Residing in the large volume and the weak coupling limit, it is straightforward for this model to satisfy condition (4.1) and we obtain $\delta_\xi \sim \mathcal{O}(10^{-4})$ and $\delta_{\tau_i} \sim \mathcal{O}(10^{-5})$.

Slow-roll dynamics of the fields

We numerically evolve the set of equations presented in (4.5) with the values of the model parameters and initial conditions presented in table 3. We are focusing on vanishing initial velocities for the inflatons *i.e.* $\{\varphi'_1(0), \varphi'_2(0), \varphi'_3(0)\} = 0$.



⁶Note that, we do not intend to study the reheating dynamics in this article

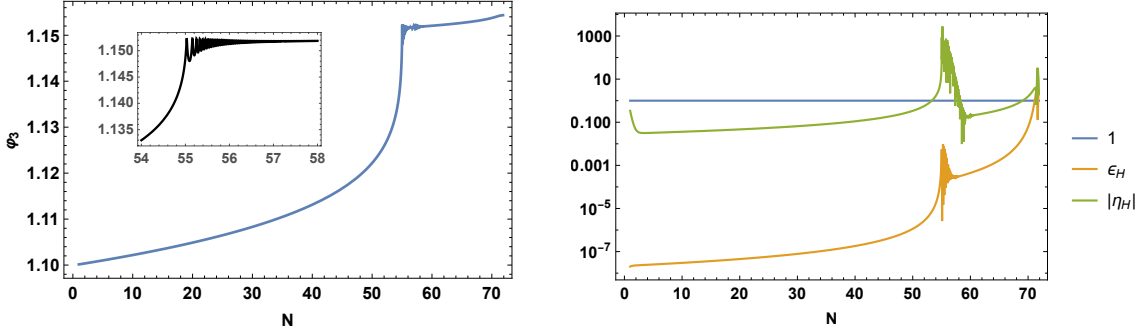


Figure 4: Field evolutions of the three canonical scalar fields. ϵ_H stays less than 1 throughout the evolution but η_H crosses 1 at $N = 60$. The reason for the same have been explained in the text.

If we assess the initial conditions for the inflatons and their respective minima in table 3, we see that the initial path of the inflationary trajectory starts on the left side of $\langle\varphi_1\rangle$ and $\langle\varphi_2\rangle$. While both (φ_1, φ_2) are displaced away from their minima, if we choose φ_3 close to its minimum, we obtain an interesting three-field attractor where all three-fields move together to give sufficient amount of e-folds. As soon as the fields settle at their minima, inflation ends. In Figure 4, although along φ_1 and φ_2 the displacement in fields ($\Delta\varphi_{1,2}$) remain relatively small in most of their evolution, they do exhibit some movement, as evident from the inset image. The potential along the φ_3 is the steepest among the rest, it dominates the field trajectory in the beginning when the (φ_1, φ_2) move relatively slower. Hence, we may conclude that most of the slow-roll dynamics upto $N = 55$ is mostly a cumulative effect of these fields with contributions from φ_3 being the dominant one. An interesting observation here is that, although Table 4 shows that φ_3 has the lowest mass at the global minimum, as the inflaton evolves from a shifted position, this hierarchy reverses, making φ_3 the steepest among all.

The trajectory of φ_3 shows a peculiar behavior because if we notice and compare between the path φ_3 follows and its value of the minimum from table 3 then we can see that they are not in accordance. Roughly $N = 55$ onwards, we notice vigorous oscillations in both ϵ_H, η_H followed by a softening where η_H returns to slow-roll after a brief period of slow-roll violation. We have $\epsilon_H < 1$ throughout but its amplitude increases beyond $N = 55$. The oscillation in (ϵ_H, η_H) is a manifestation of the oscillation in φ_3 direction around $N \sim 55$.

We can understand this behavior by looking at the field trajectories as well as the steepness of the potential along φ_3 . The reason is φ_3 falls in a ridge of the potential. We notice that along the inflationary trajectory where (φ_1, φ_2) are far away from their minima, the true minimum for φ_3 disappears and the ridge becomes unavoidable. Although, notice that the ridge is not at the point where the potential diverges which is at $\varphi_3 \equiv \sqrt{4/3}$. The ridge acts like a false vacuum for φ_3 and when it falls there it leads to such oscillations. Now, as soon as (φ_1, φ_2) move close to their minima along the trajectory, φ_3 recovers its actual minimum and φ_3 restarts its journey towards the true vacuum. Interestingly, it

appears that after the oscillation the fields switch their roles, (φ_1, φ_2) move faster whereas φ_3 appears relatively constant. For the last few efolds, all the fields become active to roll towards the global minimum, thereby increasing both ϵ_H and η_H , signalling the end of inflation. These behavior can also be seen in the figure below.

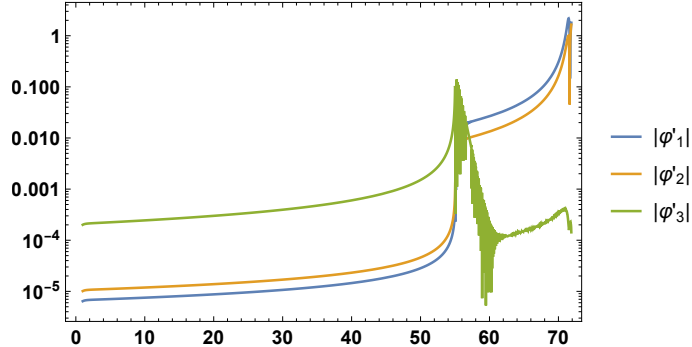


Figure 5: Velocity of the fields.

As expected, φ_3 being the steepest among them, its velocity dominates over the other and as soon as it falls off the ridge the velocity decreases but does not become zero. When φ_3 oscillates at the ridge, (φ_1, φ_2) become dominant and move towards their minimum. In summary, this attractor solution we have discovered, gives a *quasi-single-field* behavior in the first part of inflation and *quasi-double-field* for the second period of inflation. We will confirm this claim by looking at the projection of the masses of the scalar fields as well as perturbative masses of the modes throughout the inflationary evolution. We will discuss this in greater detail in the following subsections.

To complete the analysis of this section, we also confirm that our benchmark model produces the correct hierarchy of scales as shown below.

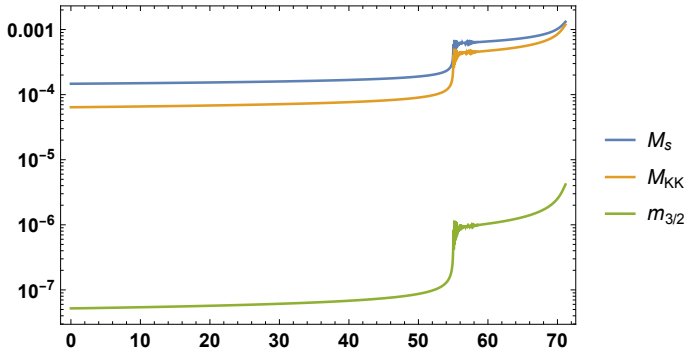


Figure 6: Correct hierarchy of mass scales where $M_s > M_{KK} > m_{3/2}$. All the masses are expressed in Planck units.

Turning rate and torsion

Depending on the nature of turns and torsions, one can get a variety of different models with different predictions for cosmological observables. Models featuring sharp turns [75],

smooth and large turns [76], and turns combined with non-planar motion [60, 63] have proven useful in the study of primordial black holes and particle production. For our multi-field canonical model with vanishing Ricci curvature, it is expected that the fields follow a geodesic ($\mathcal{D}_t T = 0$) for most of its evolution producing small $\Omega/H \sim \mathcal{O}(10^{-8})$ and $\tau \sim \mathcal{O}(10^{-12})$. During the crossing of pivot-scale ($k_* = 0.05 \text{ Mpc}^{-1}$) which roughly corresponds to a scale between $(N_{\epsilon_H=1} - 60) = 11.15$ to $(N_{\epsilon_H=1} - 50) = 21.15$, $(\Omega/H, \tau)$ remain small, however if we look at figure 7, we notice that beyond $N = 55$, both $(\Omega/H, \tau)$ get an enhancement in magnitude. The rapid oscillation observed in the figure below arises from the oscillation in the φ_3 direction as it falls into its false vacuum (the ridge), as we can observe in figure 4.

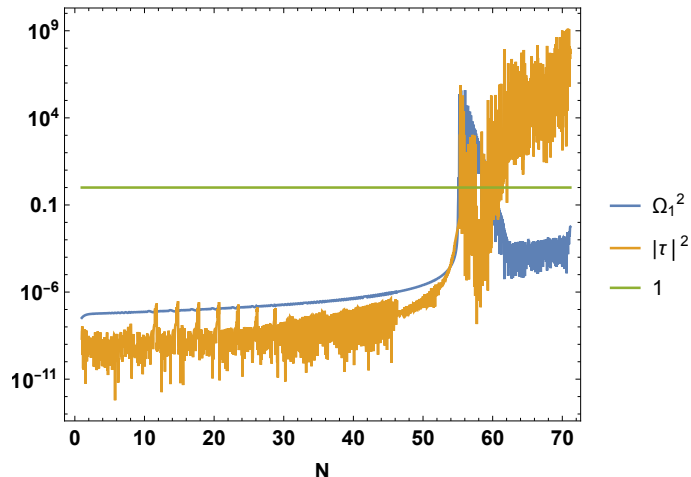


Figure 7: Hierarchy of mass scales

The oscillations are present in both Ω/H and τ direction but notice that post-oscillation the hierarchy between the torsion and the turning rate changes. This signals the fact that, the field-motion was confined within a geodesic trajectory dominated by the φ_3 field but as soon as (φ_1, φ_2) find the valley towards its minima and start their journey, the whole inflationary trajectory becomes non-planar.

4.2 Cosmological parameters

The dynamics of the linear perturbation and cosmological predictions for an inflationary model depend on the hierarchies of the adiabatic and the entropic modes. The value of $(\Omega/H, \tau)$ play a pivotal role in understanding how much entropic perturbations affect the adiabatic curvature perturbation. As we can see from the set of equations (3.11), $\tau \sim 0$ will simplify them to the standard Mukhanov-Sasaki mode equations in terms of two canonically normalised fields v_σ and v_s which depend on (Q_T, Q_N) in the following way:

$$v_\sigma = aQ_\sigma, \quad v_s = aQ_N. \quad (4.6)$$

In terms of these new variables, the mode equations in conformal time can be written as:

$$v''_{\sigma} - \xi' v'_{\sigma} + \left(k^2 - \frac{z''}{z}\right) v_{\sigma} - \frac{(z\xi')'}{z} v_s = 0, \quad (4.7)$$

$$v''_s + \xi' v'_s + \left(k^2 - \frac{a''}{a} + a^2 \mu_s^2\right) v_s - \frac{z'}{z} \xi' v_{\sigma} = 0, \quad z = a\dot{\varphi}/H. \quad (4.8)$$

$\xi' = 2a\Omega$ sources the coupling between curvature and entropic mode. $\Omega \sim 0$ naturally makes the coupling weak in our case. The masses of adiabatic and entropic perturbations can be derived from both (3.12) and the matrix (3.10). These quantities play a crucial role in determining the extent to which entropic perturbations influence inflationary perturbations, guiding us either deeper into a multi-field regime or away from it. The masses are defined as follows:

$$\frac{m_T^2}{H^2} \equiv -\frac{3}{2}\eta - \frac{1}{4}\eta^2 + \frac{1}{2}\epsilon\eta - \frac{1}{2}\frac{\dot{\eta}}{H}, \quad \cdot = \frac{d}{dt}, \quad (4.9)$$

$$\frac{M^2}{H^2} = \frac{V_{NN}}{H^2} + M_{pl}^2 \epsilon \mathbb{R} - \Omega_1^2, \quad (4.10)$$

$$\mathbb{R}_{bcd}^a = \Gamma_{bd,c}^a - \Gamma_{bc,d}^a + \Gamma_{ce}^a \Gamma_{bd}^e - \Gamma_{de}^a \Gamma_{bc}^e, \quad (4.11)$$

Below, we show a plot of (m_T^2, M^2) together with the mass along the binormal unit vector \mathcal{M}_{BB}^2 and an effective entropy mass given as $\mathcal{M}_{eff}^2 = M^2 + 4\Omega^2$:

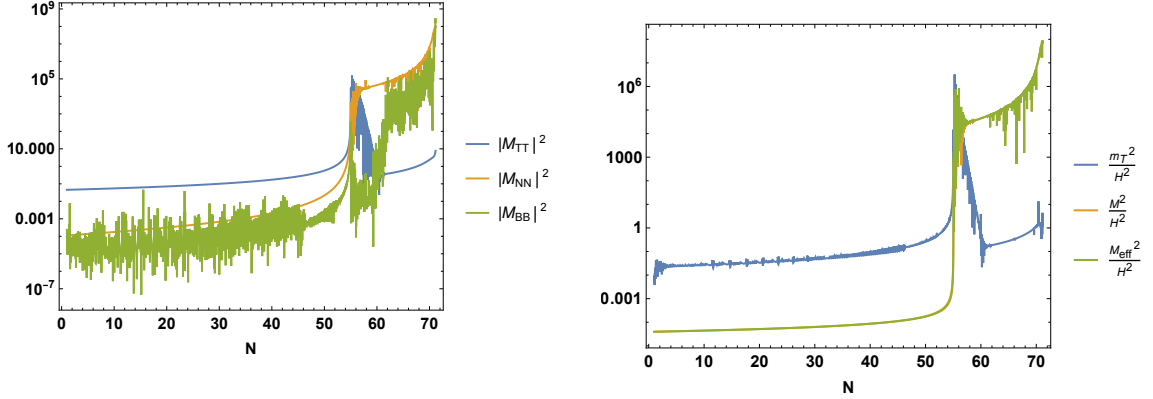


Figure 8: Left: the adiabatic mass is bigger than the entropic ones: $M_{TT} > M_{NN} > M_{BB}$. **Right:** similar hierarchy of scales are restored when the torsion is negligible. Also note that, we obtain $\mathcal{M}/\mathcal{M}_{eff} \sim 1$.

The masses also help to define a speed of sound for the adiabatic perturbations via the relation [66, 77, 78]:

$$c_s^{-2} = \frac{\mathcal{M}_{eff}^2}{M^2}.$$

We find that $\mathcal{M}_{eff} \sim M$, leading to $c_s \sim 1$ along the entire inflationary trajectory. Consequently, this results in negligible equilateral-type non-Gaussianity, with $f_{NL} \sim \mathcal{O}(10^{-8})$, as

given by the relation in [60]:

$$f_{NL} = \frac{125}{108} \frac{\epsilon_H}{c_s^2} + \frac{5}{81} \frac{c_s^2}{2} \left(1 - \frac{1}{c_s^2}\right)^2 + \frac{35}{108} \left(1 - \frac{1}{c_s^2}\right). \quad (4.12)$$

After carefully assessing the mass-scales, we also move on to checking the adiabaticity condition [78]:

$$\mathcal{A} = \left| \frac{\dot{\Omega}}{M\Omega} \right| \ll 1, \quad (4.13)$$

which holds in our case with $\mathcal{A} \sim \mathcal{O}(10^{-5})$. Therefore, given the small value of \mathcal{A} as well as the mass of the adiabatic perturbation being the dominant one, we use the standard formulae for the cosmological parameters in terms of the slow-roll parameters (3.5),

$$n_s = 1 - 2\epsilon_H - \eta_H, \quad r = 16\epsilon_H. \quad (4.14)$$

The amplitude of the power spectrum is given by,

$$\Delta_s^2 = \frac{1}{8\pi^2} \frac{H^2}{\epsilon}, \quad \Delta_t^2 = \frac{2H^2}{\pi^2}. \quad (4.15)$$

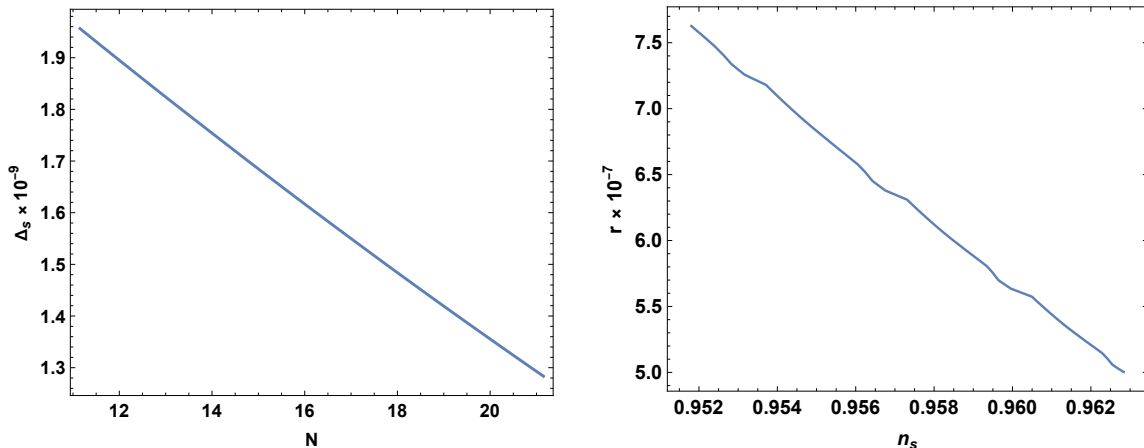


Figure 9: All the quantities are calculated at horizon crossing, which is roughly 50 – 60 e-folds before the end of inflation which is at $N_{\epsilon_H=1} = 71.15$.

The figure above confirms that we are fairly within the Planck’s bound presented in (4.4). The small value of r is a manifestation of the smallness of the scale of the potential in Planck units. Since r is directly related to the field excursion through Lyth bound, in our case, we also expect small field excursions. This makes our model in accordance with the swampland distance conjecture [79]. The running of the spectral index for this model, α_s is of the order $\mathcal{O}(10^{-3})$.

Large turns and torsions on small scales

Before ending this section, let us drop our final remark on the implications of the enhancement in the magnitude of turning rate and torsion as has been shown in figure 7. It is widely known in the literature [75, 76, 80, 81] that models for which second slow-roll parameters *i.e.* η_H is larger than ϵ_H , it can potentially give rise to efficient production of primordial black holes. The field behavior reflected in our model reveals a similar behavior like double-inflation. In double inflation, the process occurs in two stages. Initially, one field rolls down to its minimum while the second field remains frozen. In the later stage, the frozen field begins to roll, ultimately reaching its minimum and bringing inflation to an end. Similarly, in the case of the three-field inflation discussed in this paper, we observe a quasi-double inflation behavior, where the first phase of inflation is mostly driven by one field, while the second phase is governed by the other two fields as we can observe in figure 4. Although, in this case, the first phase of slow-roll takes place along the steep direction of the potential.

Referring to figure 8, we observe that during horizon crossing ($11.15 < N < 21.15$), the mass of the adiabatic mode, denoted as $\{M_{TT}^2, m_T^2\}$, remains dominant. But on a smaller scale however, when the inflationary trajectory enters its second phase, characterized by two-field dynamics, where (φ_1, φ_2) becomes more active compared to φ_3 – the masses of the entropic perturbations become dominant. This implies that the effects of turns and torsions must be accounted for, requiring a simultaneous analysis of both adiabatic and all entropic perturbations to determine the power spectrum of scalar and tensor modes. This highlights one of the most significant aspects of our paper.

Primordial black holes, considered potential progenitors of dark matter, have been widely studied in recent years, including a recent investigation within a three-field model in [63] where the authors presented a toy model. We emphasize that our work is *among the first to explore a three-field inflation scenario with non-trivial features at small scales – motivated by type-IIB string theory flux compactification where our inflatons are four-cycles of a K3-fibred Calabi-Yau*. The potential is a combination of leading order and one sub-leading terms in the inverse string expansion, and 1-loop correction terms. To ensure a nearly Minkowskian global minimum, a constant term has also been added. The fields are canonical and dimensionless in Planck units. We have done a thorough consistency checks to ensure the reliability of the 4d EFT. We plan to revisit the detailed study of primordial black holes as well as secondary induced gravitational waves in a forthcoming companion paper.

5 Conclusions

In this paper, we have presented a string motivated three-field inflationary construction for the first time where the hierarchy between first and second slow-roll parameters become evident. The second slow-roll parameter dominates the first one, clearly hinting towards non-trivial dynamics at small scales – at the same time being consistent with Planck data at the horizon crossing. The scalar potential also deviates from the usual pLVS [35] or fibre inflationary setup by their interplay between subleading corrections. The analysis is focused on the implications of the logarithmic loop corrections in the stabilization procedure, where

the subleading F^4 higher derivative corrections were utilized to uplift the flat direction. We also added a small uplifting term to ensure the presence of a Minkowski vacuum.

The above method is compatible with the large volume scenario (LVS) in which the compactification volume is stabilized to large values of order $> \mathcal{O}(10^6)$ in accordance with the semi-classical approximation and trust the underlying 4D EFT. The model reflects the correct hierarchy of mass scales, *i.e.* $M_{pl} > M_s > M_{KK} > M_{inf}$ in all the benchmark models displayed. As far as the inflationary setup is concerned, we present a multi-field inflation model where all the scalar fields are active during inflation. The inflation takes place along $(\varphi_1, \varphi_2, \varphi_3)$ directions which span the canonical basis constructed out of several four-cycle volume of the fibre modulus τ_7 , the volume of the base τ_6 and the blow-up modulus τ_1 . The three-dimensional scalar potential, defined in a canonical basis within the scalar field space, is sufficiently flat to sustain the necessary number of e-folds. Inflation starts at a position where all the scalars are shifted from their global minimum. However, it features a ridge-valley along the φ_3 direction when the other fields are away from their minimum. The potential along that direction becomes steeper than the other two directions (φ_1, φ_2) .

The minimum along φ_3 vanishes at $\{\varphi_1^{\text{shifted}}, \varphi_2^{\text{shifted}}\}$ forcing φ_3 to fall into the ridge and oscillate there – acting like a false vacuum for φ_3 . In the second stage, as φ_3 stops its oscillation, the other two fields start its journey with more kinetic energy towards their minima. As the value of (φ_1, φ_2) start to get near their minima, the true minimum for φ_3 is restored and φ_3 slowly transitions there as we can see in figure 5. This oscillation exhibits a non-trivial feature to which we now turn our attention. Due to the flat metric, as expected, throughout the slow-roll evolution, the model exhibits minor deviation from a geodesic trajectory. However, when φ_3 oscillates and the other two fields start to roll, it leads to high value of turing rate. The torsion which takes care of how much non-planar behavior is present in the trajectory, despite being small for most of the evolution, increases right after the onset of oscillation.

We can notice the same even at the level of the masses of the adiabatic and entropic modes— they switch their roles as can be seen in figure 8. The domination of entropic mass at small scales indicates the fact that at the level of perturbation, three field analysis will become unavoidable. This type of features are closely related to the production of primordial black holes at small scales – at the time of radiation domination. Besides, it can also lead to non-trivial footprint on the scalar induced gravitational waves. We plan to return to this detailed study in a companion paper. We emphasize that this trajectory is very generic for this class of models, depending on the initial condition one can easily achieve this three-field attractor.

The inflationary model presented in this paper is consistent with the data, however it has a few areas for further refinement. The value of the blow-up divisor at its minimum is large compared to the overall volume. However, we have made sure that the model still resides in the large volume regime. Note that, this is not the case for the dS models presented in table 1-2. The inflationary model is chosen so that the amplitude of the power spectrum is obtained without any fine-tuning or artificial scaling. Besides, the Kaluza-Klein and the string mass scales are almost comparable to each other in all the models— pushing us to the boundary of parametric control.

Many challenges remain as open questions with respect to the dynamics of this class of inflationary models. The exact computation of the values of χ and λ is needed to unravel the robustness of the inflationary trajectories against additional string loop effects [82]. An advantage of the proposed model is that it manages to have the EFT under control, despite the fact that it lacks an explicit mechanism of uplifting the vacuum to dS space. It would be worth studying the effects of the $\overline{D3}$ uplifting method [58] in the presence of the logarithmic loop corrections. We save these questions for a future work.

Acknowledgments

We thank George Leontaris, Pramod Shukla, and Ivonne Zavala for useful discussions and comments.

References

- [1] A. H. Guth, “The Inflationary Universe: A Possible Solution to the Horizon and Flatness Problems”, *Phys.Rev.* **D23** (1981) 347–356.
- [2] A. D. Linde, “A New Inflationary Universe Scenario: A Possible Solution of the Horizon, Flatness, Homogeneity, Isotropy and Primordial Monopole Problems”, *Phys.Lett.* **B108** (1982) 389–393.
- [3] A. Albrecht and P. J. Steinhardt, “Cosmology for Grand Unified Theories with Radiatively Induced Symmetry Breaking”, *Phys.Rev.Lett.* **48** (1982) 1220–1223.
- [4] **Planck** Collaboration, Y. Akrami *et al.*, “Planck 2018 results. X. Constraints on inflation”, *Astron. Astrophys.* **641** (2020) A10, [arXiv:1807.06211 \[astro-ph.CO\]](#).
- [5] C. Vafa, “The String landscape and the swampland”, [arXiv:hep-th/0509212](#).
- [6] G. Obied, H. Ooguri, L. Spodyneiko, and C. Vafa, “De Sitter Space and the Swampland”, [arXiv:1806.08362 \[hep-th\]](#).
- [7] P. Agrawal, G. Obied, P. J. Steinhardt, and C. Vafa, “On the Cosmological Implications of the String Swampland”, *Phys. Lett. B* **784** (2018) 271–276, [arXiv:1806.09718 \[hep-th\]](#).
- [8] E. Palti, “The Swampland: Introduction and Review”, *Fortsch. Phys.* **67** (2019) no. 6, 1900037, [arXiv:1903.06239 \[hep-th\]](#).
- [9] A. Achúcarro and G. A. Palma, “The string swampland constraints require multi-field inflation”, *JCAP* **02** (2019) 041, [arXiv:1807.04390 \[hep-th\]](#).
- [10] **CMB-S4** Collaboration, K. N. Abazajian *et al.*, “CMB-S4 Science Book, First Edition”, [arXiv:1610.02743 \[astro-ph.CO\]](#).
- [11] T. Essinger-Hileman, A. Ali, M. Amiri, J. W. Appel, D. Araujo, C. L. Bennett, F. Boone, M. Chan, H.-M. Cho, D. T. Chuss, F. Colazo, E. Crowe, K. Denis, R. Dünner, J. Eimer, D. Gothe, M. Halpern, K. Harrington, G. C. Hilton, G. F. Hinshaw, C. Huang, K. Irwin, G. Jones, J. Karakla, A. J. Kogut, D. Larson, M. Limon, L. Lowry, T. Marriage, N. Mehrle, A. D. Miller, N. Miller, S. H. Moseley, G. Novak, C. Reintsema, K. Rostem, T. Stevenson, D. Towner, K. U-Yen, E. Wagner, D. Watts, E. J. Wollack, Z. Xu, and L. Zeng, “**CLASS: the cosmology large angular scale surveyor**”, in *Millimeter, Submillimeter, and Far-Infrared Detectors and Instrumentation for Astronomy VII*, W. S. Holland and J. Zmuidzinas, eds.,

- vol. 9153 of *Society of Photo-Optical Instrumentation Engineers (SPIE) Conference Series*, p. 91531I. July, 2014. [arXiv:1408.4788 \[astro-ph.IM\]](#).
- [12] T. Matsumura *et al.*, “Mission design of LiteBIRD”, *J. Low Temp. Phys.* **176** (2014) 733, [arXiv:1311.2847 \[astro-ph.IM\]](#).
- [13] **Simons Observatory** Collaboration, P. Ade *et al.*, “The Simons Observatory: Science goals and forecasts”, *JCAP* **02** (2019) 056, [arXiv:1808.07445 \[astro-ph.CO\]](#).
- [14] **DESI** Collaboration, A. Aghamousa *et al.*, “The DESI Experiment Part I: Science, Targeting, and Survey Design”, [arXiv:1611.00036 \[astro-ph.IM\]](#).
- [15] **LSST Science, LSST Project** Collaboration, P. A. Abell *et al.*, “LSST Science Book, Version 2.0”, [arXiv:0912.0201 \[astro-ph.IM\]](#).
- [16] L. Amendola *et al.*, “Cosmology and fundamental physics with the Euclid satellite”, *Living Rev. Rel.* **21** (2018) no. 1, 2, [arXiv:1606.00180 \[astro-ph.CO\]](#).
- [17] S. Camera, M. G. Santos, and R. Maartens, “Probing primordial non-Gaussianity with SKA galaxy redshift surveys: a fully relativistic analysis”, *Mon. Not. Roy. Astron. Soc.* **448** (2015) no. 2, 1035–1043, [arXiv:1409.8286 \[astro-ph.CO\]](#). [Erratum: *Mon. Not. Roy. Astron. Soc.* 467, 1505–1506 (2017)].
- [18] P. D. Meerburg *et al.*, “Primordial Non-Gaussianity”, *Bull. Am. Astron. Soc.* **51** (2019) no. 3, 107, [arXiv:1903.04409 \[astro-ph.CO\]](#).
- [19] M. Cicoli, J. P. Conlon, A. Maharana, S. Parameswaran, F. Quevedo, and I. Zavala, “String cosmology: From the early universe to today”, *Phys. Rept.* **1059** (2024) 1–155, [arXiv:2303.04819 \[hep-th\]](#).
- [20] S. Kachru, R. Kallosh, A. D. Linde, and S. P. Trivedi, “De Sitter vacua in string theory”, *Phys. Rev. D* **68** (2003) 046005, [arXiv:hep-th/0301240](#).
- [21] J. Polchinski, “Brane/antibrane dynamics and KKLT stability”, [arXiv:1509.05710 \[hep-th\]](#).
- [22] F. F. Gautason, V. Van Hemelryck, T. Van Riet, and V. Venken, “A 10d view on the KKLT AdS vacuum and uplifting”, *JHEP* **06** (2020) 074, [arXiv:1902.01415 \[hep-th\]](#).
- [23] Y. Hamada, A. Hebecker, G. Shiu, and P. Soler, “Understanding KKLT from a 10d perspective”, *JHEP* **06** (2019) 019, [arXiv:1902.01410 \[hep-th\]](#).
- [24] A. Linde, “KKLT without AdS”, *JHEP* **05** (2020) 076, [arXiv:2002.01500 \[hep-th\]](#).
- [25] L. Randall, “The Boundaries of KKLT”, *Fortsch. Phys.* **68** (2020) no. 3-4, 1900105, [arXiv:1912.06693 \[hep-th\]](#).
- [26] R. Blumenhagen, D. Kläwer, and L. Schlechter, “Swampland Variations on a Theme by KKLT”, *JHEP* **05** (2019) 152, [arXiv:1902.07724 \[hep-th\]](#).
- [27] D. Andriot, P. Marconnet, and T. Wrase, “New de Sitter solutions of 10d type IIB supergravity”, *JHEP* **08** (2020) 076, [arXiv:2005.12930 \[hep-th\]](#).
- [28] H. Abe, T. Higaki, and T. Kobayashi, “KKLT type models with moduli-mixing superpotential”, *Phys. Rev. D* **73** (2006) 046005, [arXiv:hep-th/0511160](#).
- [29] F. Carta, J. Moritz, and A. Westphal, “Gaugino condensation and small uplifts in KKLT”, *JHEP* **08** (2019) 141, [arXiv:1902.01412 \[hep-th\]](#).

- [30] J. P. Conlon, F. Quevedo, and K. Suruliz, “Large-volume flux compactifications: Moduli spectrum and D3/D7 soft supersymmetry breaking”, *JHEP* **08** (2005) 007, [arXiv:hep-th/0505076](#).
- [31] V. Balasubramanian, P. Berglund, J. P. Conlon, and F. Quevedo, “Systematics of moduli stabilisation in Calabi-Yau flux compactifications”, *JHEP* **03** (2005) 007, [arXiv:hep-th/0502058](#).
- [32] C. P. Burgess, R. Kallosh, and F. Quevedo, “De Sitter string vacua from supersymmetric D terms”, *JHEP* **10** (2003) 056, [arXiv:hep-th/0309187](#).
- [33] D. Cremades, M. P. Garcia del Moral, F. Quevedo, and K. Suruliz, “Moduli stabilisation and de Sitter string vacua from magnetised D7 branes”, *JHEP* **05** (2007) 100, [arXiv:hep-th/0701154](#).
- [34] I. Antoniadis, Y. Chen, and G. K. Leontaris, “Logarithmic loop corrections, moduli stabilisation and de Sitter vacua in string theory”, *JHEP* **01** (2020) 149, [arXiv:1909.10525 \[hep-th\]](#).
- [35] I. Antoniadis, Y. Chen, and G. K. Leontaris, “Perturbative moduli stabilisation in type IIB/F-theory framework”, *Eur. Phys. J. C* **78** (2018) no. 9, 766, [arXiv:1803.08941 \[hep-th\]](#).
- [36] V. Basiouris and G. K. Leontaris, “Note on de Sitter vacua from perturbative and non-perturbative dynamics in type IIB/F-theory compactifications”, *Phys. Lett. B* **810** (2020) 135809, [arXiv:2007.15423 \[hep-th\]](#).
- [37] V. Basiouris and G. K. Leontaris, “Remarks on the Effects of Quantum Corrections on Moduli Stabilization and de Sitter Vacua in Type IIB String Theory”, *Fortsch. Phys.* **70** (2022) no. 2-3, 2100181, [arXiv:2109.08421 \[hep-th\]](#).
- [38] G. K. Leontaris and P. Shukla, “Stabilising all Kähler moduli in perturbative LVS”, *JHEP* **07** (2022) 047, [arXiv:2203.03362 \[hep-th\]](#).
- [39] M. Dine and N. Seiberg, “Is the Superstring Weakly Coupled?”, *Phys. Lett. B* **162** (1985) 299–302.
- [40] E. Witten, “Nonperturbative superpotentials in string theory”, *Nucl. Phys. B* **474** (1996) 343–360, [arXiv:hep-th/9604030](#).
- [41] S. Bera, D. Chakraborty, G. K. Leontaris, and P. Shukla, “Inflating in perturbative LVS: global embedding and robustness”, *JCAP* **09** (2024) 004, [arXiv:2405.06738 \[hep-th\]](#).
- [42] M. Cicoli, C. P. Burgess, and F. Quevedo, “Fibre Inflation: Observable Gravity Waves from IIB String Compactifications”, *JCAP* **03** (2009) 013, [arXiv:0808.0691 \[hep-th\]](#).
- [43] M. Cicoli, F. Muia, and P. Shukla, “Global Embedding of Fibre Inflation Models”, *JHEP* **11** (2016) 182, [arXiv:1611.04612 \[hep-th\]](#).
- [44] M. Cicoli, D. Ciupke, V. A. Diaz, V. Guidetti, F. Muia, and P. Shukla, “Chiral Global Embedding of Fibre Inflation Models”, *JHEP* **11** (2017) 207, [arXiv:1709.01518 \[hep-th\]](#).
- [45] K. Becker, M. Becker, M. Haack, and J. Louis, “Supersymmetry breaking and alpha-prime corrections to flux induced potentials”, *JHEP* **06** (2002) 060, [arXiv:hep-th/0204254](#).
- [46] I. Antoniadis, S. Ferrara, R. Minasian, and K. S. Narain, “R⁴ couplings in M and type II theories on Calabi-Yau spaces”, *Nucl. Phys. B* **507** (1997) 571–588, [arXiv:hep-th/9707013](#).

- [47] I. Antoniadis, R. Minasian, and P. Vanhove, “Noncompact Calabi-Yau manifolds and localized gravity”, *Nucl. Phys. B* **648** (2003) 69–93, [arXiv:hep-th/0209030](#).
- [48] I. Antoniadis, R. Minasian, S. Theisen, and P. Vanhove, “String loop corrections to the universal hypermultiplet”, *Class. Quant. Grav.* **20** (2003) 5079–5102, [arXiv:hep-th/0307268](#).
- [49] M. Cicoli and F. Quevedo, “String moduli inflation: An overview”, *Class. Quant. Grav.* **28** (2011) 204001, [arXiv:1108.2659 \[hep-th\]](#).
- [50] S. Bera, D. Chakraborty, G. K. Leontaris, and P. Shukla, “Global embedding of fiber inflation in a perturbative large volume scenario”, *Phys. Rev. D* **110** (2024) no. 10, 106009, [arXiv:2406.01694 \[hep-th\]](#).
- [51] M. Kreuzer and H. Skarke, “Complete classification of reflexive polyhedra in four-dimensions”, *Adv. Theor. Math. Phys.* **4** (2000) 1209–1230, [arXiv:hep-th/0002240](#).
- [52] R. Altman, J. Gray, Y.-H. He, V. Jejjala, and B. D. Nelson, “A Calabi-Yau Database: Threefolds Constructed from the Kreuzer-Skarke List”, *JHEP* **02** (2015) 158, [arXiv:1411.1418 \[hep-th\]](#).
- [53] M. B. Green and P. Vanhove, “D instantons, strings and M theory”, *Phys. Lett. B* **408** (1997) 122–134, [arXiv:hep-th/9704145](#).
- [54] M. Bianchi, A. Collinucci, and L. Martucci, “Magnetized E3-brane instantons in F-theory”, *JHEP* **12** (2011) 045, [arXiv:1107.3732 \[hep-th\]](#).
- [55] M. Cvetič, R. Donagi, J. Halverson, and J. Marsano, “On Seven-Brane Dependent Instanton Prefactors in F-theory”, *JHEP* **11** (2012) 004, [arXiv:1209.4906 \[hep-th\]](#).
- [56] R. Blumenhagen, S. Moster, and E. Plauschinn, “Moduli Stabilisation versus Chirality for MSSM like Type IIB Orientifolds”, *JHEP* **01** (2008) 058, [arXiv:0711.3389 \[hep-th\]](#).
- [57] D. Ciupke, J. Louis, and A. Westphal, “Higher-Derivative Supergravity and Moduli Stabilization”, *JHEP* **10** (2015) 094, [arXiv:1505.03092 \[hep-th\]](#).
- [58] M. Cicoli, A. Grassi, O. Lacombe, and F. G. Pedro, “Chiral global embedding of Fibre Inflation with $\overline{D3}$ uplift”, [arXiv:2412.08723 \[hep-th\]](#).
- [59] O. Lacombe, L. Paoloni, and F. G. Pedro, “Higher-derivative supersymmetric effective field theories”, [arXiv:2409.08984 \[hep-th\]](#).
- [60] V. Aragam, S. Paban, and R. Rosati, “Multi-field Inflation in High-Slope Potentials”, *JCAP* **04** (2020) 022, [arXiv:1905.07495 \[hep-th\]](#).
- [61] P. Christodoulidis and R. Rosati, “(Slow-)twisting inflationary attractors”, *JCAP* **09** (2023) 034, [arXiv:2210.14900 \[hep-th\]](#).
- [62] V. Aragam, S. Paban, and R. Rosati, “Primordial stochastic gravitational wave backgrounds from a sharp feature in three-field inflation. Part I. The radiation era”, *JCAP* **11** (2023) 014, [arXiv:2304.00065 \[astro-ph.CO\]](#).
- [63] V. Aragam, S. Paban, and R. Rosati, “Primordial Stochastic Gravitational Wave Backgrounds from a Sharp Feature in Three-field Inflation II: The Inflationary Era”, [arXiv:2409.09023 \[astro-ph.CO\]](#).
- [64] L. Pinol, “Multifield inflation beyond $N_{\text{field}} = 2$: non-Gaussianities and single-field effective theory”, *JCAP* **04** (2021) 002, [arXiv:2011.05930 \[astro-ph.CO\]](#).

- [65] A. Achucarro, J.-O. Gong, S. Hardeman, G. A. Palma, and S. P. Patil, “Effective theories of single field inflation when heavy fields matter”, *JHEP* **05** (2012) 066, [arXiv:1201.6342 \[hep-th\]](#).
- [66] A. Achucarro, V. Atal, S. Cespedes, J.-O. Gong, G. A. Palma, and S. P. Patil, “Heavy fields, reduced speeds of sound and decoupling during inflation”, *Phys. Rev. D* **86** (2012) 121301, [arXiv:1205.0710 \[hep-th\]](#).
- [67] A. Hetz and G. A. Palma, “Sound Speed of Primordial Fluctuations in Supergravity Inflation”, *Phys. Rev. Lett.* **117** (2016) no. 10, 101301, [arXiv:1601.05457 \[hep-th\]](#).
- [68] D. I. Kaiser, E. A. Mazenc, and E. I. Sfakianakis, “Primordial Bispectrum from Multifield Inflation with Nonminimal Couplings”, *Phys. Rev. D* **87** (2013) 064004, [arXiv:1210.7487 \[astro-ph.CO\]](#).
- [69] S. Céspedes and G. A. Palma, “Cosmic inflation in a landscape of heavy-fields”, *JCAP* **10** (2013) 051, [arXiv:1303.4703 \[hep-th\]](#).
- [70] B. Valeixo Bento, D. Chakraborty, S. Parameswaran, and I. Zavala, “A guide to frames, 2π 's, scales and corrections in string compactifications”, [arXiv:2301.05178 \[hep-th\]](#).
- [71] D. Chakraborty, R. Chiovoloni, O. Loaiza-Brito, G. Niz, and I. Zavala, “Fat inflatons, large turns and the η -problem”, *JCAP* **01** (2020) 020, [arXiv:1908.09797 \[hep-th\]](#).
- [72] M. Cicoli, F. Quevedo, and R. Valandro, “De Sitter from T-branes”, *JHEP* **03** (2016) 141, [arXiv:1512.04558 \[hep-th\]](#).
- [73] S. Kachru, M. B. Schulz, P. K. Tripathy, and S. P. Trivedi, “New supersymmetric string compactifications”, *JHEP* **03** (2003) 061, [arXiv:hep-th/0211182](#).
- [74] C. Crinò, F. Quevedo, and R. Valandro, “On de Sitter String Vacua from Anti-D3-Branes in the Large Volume Scenario”, *JHEP* **03** (2021) 258, [arXiv:2010.15903 \[hep-th\]](#).
- [75] N. Parra, S. Sypsas, G. A. Palma, and C. Zenteno, “Particle creation from non-geodesic trajectories in multifield inflation”, [arXiv:2410.13843 \[hep-th\]](#).
- [76] R. Ishikawa and S. V. Ketov, “Exploring the parameter space of modified supergravity for double inflation and primordial black hole formation”, *Class. Quant. Grav.* **39** (2022) no. 1, 015016, [arXiv:2108.04408 \[astro-ph.CO\]](#).
- [77] A. Achucarro, J.-O. Gong, S. Hardeman, G. A. Palma, and S. P. Patil, “Features of heavy physics in the CMB power spectrum”, *JCAP* **01** (2011) 030, [arXiv:1010.3693 \[hep-ph\]](#).
- [78] S. Cespedes, V. Atal, and G. A. Palma, “On the importance of heavy fields during inflation”, *JCAP* **05** (2012) 008, [arXiv:1201.4848 \[hep-th\]](#).
- [79] H. Ooguri, E. Palti, G. Shiu, and C. Vafa, “Distance and de Sitter Conjectures on the Swampland”, *Phys. Lett. B* **788** (2019) 180–184, [arXiv:1810.05506 \[hep-th\]](#).
- [80] M. Braglia, D. K. Hazra, F. Finelli, G. F. Smoot, L. Sriramkumar, and A. A. Starobinsky, “Generating PBHs and small-scale GWs in two-field models of inflation”, *JCAP* **08** (2020) 001, [arXiv:2005.02895 \[astro-ph.CO\]](#).
- [81] G. A. Palma, S. Sypsas, and C. Zenteno, “Seeding primordial black holes in multifield inflation”, *Phys. Rev. Lett.* **125** (2020) no. 12, 121301, [arXiv:2004.06106 \[astro-ph.CO\]](#).
- [82] X. Gao, A. Hebecker, S. Schreyer, and V. Venken, “Loops, local corrections and warping in the LVS and other type IIB models”, *JHEP* **09** (2022) 091, [arXiv:2204.06009 \[hep-th\]](#).